AN NMR STUDY ON SOLVENT-POLYMER INTERACTIONS

AN NMR STUDY

ON

SOLVENT-POLYMER INTERACTIONS

By

STEPHEN HUGHES, B.Sc.

A Thesis

Submitted to the School of Graduate Studies

in Partial Fulfilment of the Requirements

for the Degree

Master of Science

McMaster University

MASTER OF SCIENCE (1991) **McMASTER UNIVERSITY**

(Chemistry) Hamilton, Ontario

TITLE: An NMR Study on Solvent-Polymer Interactions

AUTHOR: Stephen Hughes, B.Sc. (University of P.E.I.)

SUPERVISOR: Professor A.D. Bain

NUMBER OF PAGES: xii, 81

ABSTRACT

Approximately 80 percent of all synthetic polymers used are cross-linked polymers, unfortunately the characterization of cross-linked polymers has not kept up with their use. This study tries to help in the characterization of cross-linked polymer systems. More specifically the interactions of cross-linked polymer systems with solvents will be probed. Nuclear Magnetic Resonance (NMR) spectrometric techniques will be used to characterize solvent-polymer interactions.

The cross-linked polymer system studied was the polymer ethylene glycol dimethacrylate (EGDMA) with methylmethacrylate (MMA). A splitting of the solvent signals was observed in the NMR spectrum which can be used to understand these solvent-polymer interactions. Several NMR parameters and swelling of the polymers were measured in order to understand these interactions. The chemical shift differences between the solvent types and the peak linewidths were measured. As the polymer becomes more highly cross-linked the chemical shift differences and the linewidths increases. This compactness can be monitored by measuring the degree of swelling of the polymer. In addition the possibility of an isotope effect was explored by monitored by placing the polymer in solvent mixture of $CHCl_3/CDCl_3$ and varying the temperature. No isotope dependence was found to exist for chloroform over the temperature range analyzed. The degree of splitting and the occurrence of splitting was found to be dependent on the solvent system. In general, solvent splitting is present for solvents that are able to cause the polymer to swell appreciably. For 4.8 weight percent EGDMA in

EGDMA/MMA polymer a splitting is usually observed for a solvent that is able to swell the polymer to twice its dry size. The association between the solvents and the polymers can be best explained by breaking the interactions into a number of components.

The explanation is based on the presence of three interactions. A weak chemical interaction exists between the solvent and the polymer to account for the field dependent linewidths. A second chemical interaction that results is a binding between the solvent and the polymer and causes the solvent splitting to occur. The third interaction is a result of the increased rigidity and compactness of the polymer as the weight percent EGDMA in EGDMA/MMA polymer increases. Alternatively as the polymer becomes more compact the chemical shift difference between the two types of solvents increases.

Ultimately, it is shown that NMR is a useful aid in understanding solvent-polymer interactions.

ACKNOWLEDGEMENTS

I would like to express my sincere gratitude to my supervisor Dr. A. D. Bain for his patience and understanding. I also express my thanks to the other members of the research group namely, Mr. I. Burton, Ms. J. Cramer, Mr. G. Duns, Dr. B. Fulton, Ms. L. Lai-Mui Lao and Mr. H. Tabbara. I have appreciated the warmth and laughter the research group have provided. Special thanks goes to Ms J. Cramer for her encouragement and Mr. G. Duns for his advise on NMR and research. In addition I thank Dr. T. Wildman for his words of encouragement during my first year of graduate school. Also I would like to thank Dr. H. Stöver for his help in the polymer synthesis and his discussions on polymers systems. In addition, I thank Mr. B. Sayer and Dr D. W. Hughes for their assistance on operating the NMR spectrometers.

I also thank Dr. L.F. Loucks for his understanding during my undergraduate years at U.P.E.I. Special thanks goes out to the students from Prince Edward Island particularly Ms. C. Hill, Ms G. MacEachern, and Mr. M. Walker.

Finally I would like to thank my family for their support.

TABLE OF CONTENTS

LIST OF TABLES

LIST OF FIGURES

Chapter 1

INTRODUCTION

Although Nuclear Magnetic Resonance (NMR) spectroscopy was first detected some forty-five years ago,[1,2] it still undergoes tremendous growth. This year NMR received additional recognition when Richard Ernst was awarded the Nobel Prize in Chemistry. His contributions both in theoretical and experimental NMR form the basis of Fourier transform NMR as well as 2-D and 3-D NMR techniques. NMR provides valuable information in molecular structure determination[3,4] and dynamics.[5-7] NMR has traditionally been used in chemistry (organic, inorganic, analytical and physical) and physics, and has seen increased application in polymer chemistry,[8,9] pharmaceutical applications,[10] biological,[11-14] biomedical[15-17] and material science.[11,18]

Several NMR techniques are employed for molecular structure determination and molecular dynamics. The NMR techniques involve combinations of radio-frequency pulses, time delays, selective irradiation of peaks and polarization transfer. The technique used depends on the information that is sought. The simple one pulse experiment provides the basic 1-D spectra. The only information that can be easily obtained here are chemical shifts, scalar coupling constants and integrals. The number of protons attached

to a carbon can be determined by a J-modulated spin echo sequence, and other techniques such as polarization transfer to increase the sensitivity of nuclear spin state transitions. Many other techniques are available and they can be classed as either techniques that utilize chemical shift correlations or through-space correlations.

NMR is used in polymer analysis in a number of ways.[19] It is used to study solid state NMR of polymers,[20-22] polymeric liquid crystals,[23] polymers at surfaces,[24] cross-linked polymers systems,[20,25] and conformational analysis.[26,27] By combining a number of techniques namely, proton dipolar-decoupling (DD), magic-angle sample spinning (MAS) and cross-polarization (CP), high resolution solid-state ^{13}C NMR can provide valuable information. ^{13}C NMR studies can be used to investigate the microstructure and intramolecular conformations of the polymer chains in solids. In solid-state NMR there is a significant distribution of chemical shifts for each nuclei. This distribution has an orientational dependence with respect to the applied magnetic field, and can be used to estimate the orientation of the polymer in the sample. For a recent review on high resolution solid-state NMR and a brief discussion on the techniques discussed above, one is encouraged to see the review by Laupretre.[21]

NMR of liquid crystal polymers (LCP) is usually focused on phase transitions and determining the ordering (arrangement) of the LCP. The more common techniques to probe LCP transitions are a combination of differential scanning calorimetry (DSC) and optical microscopy. Although DSC and optical microscopy techniques do provide some information on the type of mesophase present, they do not provide any dynamic information. Multinuclear NMR provides a means by which these transitions and

ordering information can be obtained. Perry and Koenig[23] provide a recent review of LCP in high resolution solid state NMR.

NMR is used mainly in cross-linked polymers systems for the characterization of the type, number and distribution of cross-links in polymeric materials. For example from the ^{13}C NMR spectra in a series of poly(styrene)-divinylbenzene gels swollen in $CDCl_3$ it was found for cross-linker density from 0.007 to 0.112 that the linewidths of aromatic carbons increase with cross-linker density.[28] NMR parameters like spin-lattice relaxation time constants, to be discussed in detail later, have been measured as a function of weight percent cross-linker. Other nuclei like ^{29}Si and ^{15}N have been used to study cross-linked systems. For a recent review on cross-linked polymers see Andreis and Koenig.[25]

In addition NMR spectra of polymers have been measured at surfaces. NMR has been used to probe the dynamics and structure of polymer species on solid surfaces. A study of the behaviour of poly(isopropyl acrylate), PIPA, on silica revealed that the solid-state ^{13}C spectrum of the surface bound species has better resolution than that of the of bulk polymer for several resonances. Another aspect of polymers at surfaces is their conformations.[24] Other polymer surface studies have attempted to determine the conformation of adsorbed polymers at the solid-liquid interface and to characterize the system after having modified the interface between the solid substrate and the polymer. A slightly different application of NMR for adsorbed polymers is based on the use of NMR solvent self diffusion coefficients to predict the drying of coatings. Although studies of polymers on surfaces have been conducted; analysis and interpretation is often very difficult.

The conformational analysis of polymers enables one to understand more fully the two and three dimensional network of the polymer system. Simple studies, by conformational standards, include determining the tacticity or stereochemical configuration of for example poly(methylmethacrylate), PMMA. The conformation studies can range from analyzing the conformation of amino acid residues, to probing enzyme substrate interactions. Many NMR techniques facilitate the determination of the conformation of large molecules for very complex systems.

For cross-linked polymer systems the usual solid-state ^{13}C NMR spectrum is typically very broad, sometimes over a few hundred kilohertz (kHz) in width. In solid state there is a number of line broadening mechanisms namely chemical shift anisotropy, chemical shift distribution and dipolar broadening. Magnetic field inhomogeneities contribute to broadening, in solid-state NMR, but only a small amount. Field inhomogeneities refers to the ability of providing an uniform magnetic field across the entire sample. In the other extreme, in solution state NMR the dipolar broadening and chemical shift anisotropy averages to zero due to rapid motion of the polymer. Thus, in order to obtain spectra of cross-linked polymers that are well resolved, one would ideally like to have a solution state sample. However, as mentioned earlier, various techniques such as magic-angle spinning, dipolar decoupling, and cross-polarization can be applied to a solid-state sample in order to eliminate most of the broadening.

For cross-linked polymer networks one can obtain reasonable detailed spectra without the aid of magic-angle spinning, dipolar decoupling, and cross-polarization. The spectra can be obtained by placing the cross-linked polymers into a solvent, and allowing

them to swell. Cross-linked polymers do not dissolve rather, they swell. The swelling of the polymer depends on the polymer system being studied, the solvent medium, and the weight percent cross-linker. The degree of swelling depends on how well the solvent and the polymer are able to interact. The theory of the swelling of the polymer will be discussed in Chapter 2. In general the swelling of the polymer decreases with increasing cross-link density.

In analyzing the ^{13}C spectrum of a cross-linked polymer system an abnormality was observed in the solvent peaks.[29] This abnormality being two solvent peak for each peak expected. It was speculated that maybe the solvent splitting could be used to characterize the polymer. Cross-linked polymers at low percentages of cross-linking can swell when placed in favourable solvents. It was noted[29] for EGDMA/MMA polymer in $CDCL_3$ that the solvent splits into two magnetically distinct signals. This solvent splitting was first noted by Gordon[30] in 1962, in the NMR spectra of water in ion-exchange resins. The recently in 1984,[31] toluene splitting was observed in cross-linked polystyrene gel beads 16-18% ring substituted with benzyl-tri-n-butylphosphonium chloride group. Only a few cases of solvent splitting have been noted, and the majority of the work has been on ion-exchange resins.

Much of the early work on the splitting of solvents in ion-exchange resin-solvent systems focused on what causes changes in the splitting.[30,32-34] The investigated resins were usually based on sulfonated cross-linked poly(styrene)-divinylbenzene(DVB) systems. The resin in an aqueous medium exhibited two peaks corresponding to protons of water molecules inside and outside the resin. The chemical shift difference between

these two sites was proportional to the molality of the resin; molality being defined as the number of moles or resin sites per kilogram of absorbed water. The greater the molality of the resin the greater the chemical shift difference. The dependence of the hydration number (simply the number of water molecules associated with an ion) and the linewidths of the peaks on the degree of cross-linking (% DVB) were also observed. It was determined for a Dowex-50W type resin with a sodium counterion,[34] that the hydration number for a resin ion was less for than that for a ion in solution. In addition the hydration number increased as the percentage DVB decreased. In this study, the ^{23}Na linewidths, at half height, increased with increasing percentage DVB cross-linker. The splitting was shown to be a sensitive probe for these systems.

One report[35] shows that the difference in chemical shift between the two types of protons in the water molecules is found to be dependent on the particle size. With decreasing particle size the chemical shift difference spacing decreases and the two peaks gradually merge until only a single peak remains. This study was on a sulfonated poly(styrene)-divinylbenzene cross-linked polymer. Two separate signals due to internal and external water were observed at room temperature for particles of a diameter larger than 10μm.[36] In addition as the temperature increased (5°C to 90°C) the particle size where the signals become one (coalescence) increases (20 to 45μm). This report, to my knowledge, is the only investigation on particle size effects, and has not been applied to other systems.

The origin of the splitting of the solvent was analyzed by Gordon.[30] Calculations of the splitting on the chemical shift difference upon the addition of polystyrene

divinylbenzene beads in water, toluene, dioxane and acetonitrile showed to a first approximation, to be in agreement with the difference in volume susceptibilities, χ_v. To my knowledge no other attempt has been made to explain the splitting effect in ion-exchange resin, most studies show dependencies between the chemical shift difference with, for example, percentage cross-linking and hydration numbers. In non-ion exchange systems Marshall and Wilson[37] described a polymer-solvent interaction which resulted in the splitting. The interaction of cured maleic anhydride polyester resins with various solvents suggested the most likely interaction was between polar regions of the swollen polymer and the polar regions of the solvents. However the exact origin of the splittings are not fully understood.

Time dependent NMR phenomena can provide further information on the characterization of cross-linked polymers. Creekmore and Reiley[38] reported an exchange rate of 0.73 sec^{-1} for water in a Dowex 50W-8X acid form resin. Also for this resin the ^1H T_1's were determined for bulk water protons and resin water protons to be 2.9 and 0.45 seconds respectively. As mentioned earlier Ford *et al*[31] analyzed toluene splitting in cross-linked polystyrene gel beads 16-18% ring substituted with benzyl-tri-n-butylphosphonium chloride. Using a selective inversion technique the exchange rates of toluene were found to be between 0.2 and 0.6 $seconds^{-1}$. Also the ^{13}C T_1's for the internal peak were always smaller than the T_1 for the exterior peak, for the methyl group, 6 and 15 seconds respectively. For the above two studies the T_1's of the internal peak are smaller than the T_1's of the exterior peak. Exchange rates as a function of percent cross-linking were investigated[39] for dichloromethane and toluene in a poly(styrene)-

divinylbenzene polymer. The trend was as the percentage cross-linking increased the slower the exchange rate. In addition an apparent linear dependence of the exchange rates on d^{-2}, inverse square of particle diameter, suggested that for toluene in 10% cross-linked polystyrene intraparticle diffusion is the rate determining step. However the exchange rates for dichloromethane in 1% cross-linked polystyrene fit neither d^{-2} nor a d^{-1} dependence, which indicates that the diffusion is controlled by both intraparticle and film diffusion. The exchange rates of the systems studied are on the order of 0.1 to 1 $second^{-1}$.

NMR will be used to analyze solvent polymer systems. The splitting will be measured as a function of the weight percent cross-linking, to see if can be used as an alternative method to measure cross-linking density. Spectra of several different nuclei will be used namely, ^{13}C, ^{1}H, and ^{2}H to carry out this study. An attempt to explain the origin of the splitting by studying the polymer in several solvent media and an attempt to generalize the interaction will be conducted. Before the results will be discussed, some basic theory on NMR relevant to the polymer-solvent analysis will be discussed.

Chapter 2

THEORY

BASIC PRINCIPLES

After an introduction to the basic phenomenon of NMR, a discussion of some aspects of NMR relevant to this work will be elaborated. General references on NMR are available,[3,5,7,40] if a more detailed discussion is needed. Magnetic susceptibility will be introduced and an expression for a correction factor will be developed. Magnetization, the NMR signal, can be easily detected and manipulated to produce the NMR spectrum. Various NMR parameters can be measured to elucidate the solvent-polymer interactions. These NMR parameters are spin-lattice relaxation time constants, linewidths and chemical shifts, In addition, the variation of the temperature can provide additional information. Also the possibility of the utilization of this technique to further characterize cross-linked polymers will be discussed. Wherever possible reference to literature will be given to provide an indication of how each of the aspects have been used or could be used to understand these solvent-polymer systems.

Nuclear magnetic resonance involves transitions between nuclear spin energy levels (see the Figure 1).

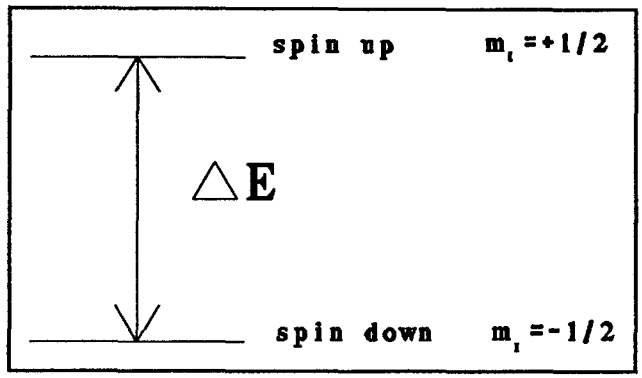

Figure 1. The figure shows the two energy levels for the nuclear spin transition for spin 1/2.

The transitions arise because the nuclei of some atoms have magnetic moments and these magnetic moments have different quantized orientations relative to the applied field for different nuclear spin states (see Figure 2a). Actually any atomic nucleus which possess either odd mass or odd atomic number, or both, has a quantized angular momentum and a magnetic moment (see Figure 2).

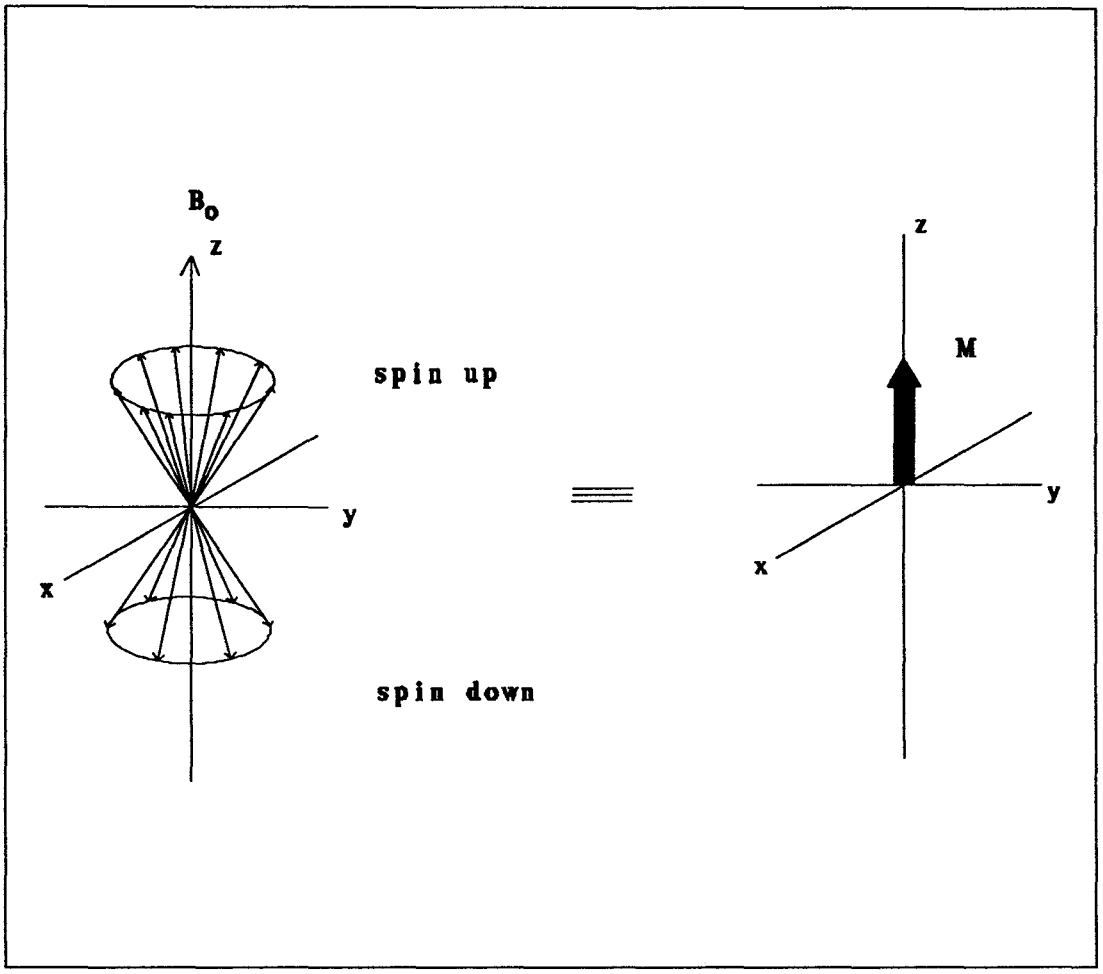

Figure 2. The figure shows how the different orientations of a spin 1/2 nucleus (left) can be viewed as vector (right).

In NMR we apply a magnetic field (B_o) along a particular direction, by convention, the z axis. For nuclei with spin, the magnetic moment vector appears to rotate around the z axis with a quantized angular momentum. In the magnetic field B_o there is a preference for one orientation of angular momentum to align with the field B_o, and one orientation to align against the field. This difference in relative orientation of spins can be represented as a vector quantity. This vector, called magnetization (M) is defined as the

total magnetic moment of the sample (see Figure 2). Magnetization will be discussed later in the relaxation and chemical exchange sections. As displayed in Figure 1 the two nuclear spin states for spin 1/2 nucleus are normally described in terms of their z-component of angular momentum. For example, for nuclear spin (I=1/2) there are two nuclear spin states, namely the z-component of angular momentum 1/2 and spin -1/2. In general, for each of the nuclei with spin, the number of allowed spin states which it may adopt is quantized and determined by its nuclear spin quantum number I. For a nucleus of spin quantum number I, there are 2I + 1 allowed nuclear spin states. Both ^{1}H and ^{13}C have spin 1/2 and therefore only have two allowed energy levels. Deuterium ^{2}H however has spin 1 and has three energy levels, their z-component of the angular momentum are +1, 0, and -1. For a more detailed discussion see Harris.[5]

For a spin 1/2 nucleus the energy difference between the two nuclear spin states is

$$\Delta E = h\nu = \gamma(h/2\pi)B_o \qquad (1)$$

h is Planck's constant
ν is frequency of radiation
γ is the magnetogyric ratio of the nucleus of interest
B_o is the strength of the magnetic field

The magnetogyric ratio (γ) is a constant for each nucleus, and it is the ratio of magnetic moment to the angular momentum. For example the magnetogyric ratio of ^{1}H, ^{2}H, ^{13}C and electron are shown below.

Particle	Spin (I)	Magnetogyric Ratio $\gamma / 10^7$ rad T^{-1} s^{-1}
^1H	1/2	26.7519
^2H	1	4.1066
^{13}C	1/2	6.7283
electron	1/2	-1.76084×10^4

Table 1. The table shows the magnetogyric ratio (γ) for the above species.

The negative sign for electrons indicates that the direction of rotation about the z axis is opposite to that for nuclei of positive γ. Further consideration of γ will be discussed later.

CHEMICAL SHIFT

In order to see the great advantage of NMR, consider a simple nucleus like the proton. The power of NMR arises because not every proton in a molecule has its transition between nuclear spin states at exactly the same frequency. This change in frequency is due to the fact that the various protons in a molecule are surrounded by a slightly different electronic environment. The protons are said to be shielded by the electrons which surround them. The magnitude of this shielding increases with increasing electron density around the protons. The resulting magnetic field that a nucleus experiences is lowered by the field that shields it. The nucleus experiences a slightly lower field and thus a lower transition frequency. This allows a means of distinguishing between various types of protons within a molecule, if the lines are very narrow. The difference in frequencies for different types of protons is very small. In practice the exact

frequency is usually not determined, but measured relative to a frequency of a reference compound. The normal way this frequency difference is expressed is in terms of chemical shift(δ). The chemical shift is defined by the shift (in Hz) of the sample (ν_{sample}) from the reference compound ($\nu_{reference}$) divided by the reference frequency (in MHz).

$$\delta = \frac{\nu_{sample}\ (Hz) - \nu_{reference}\ (Hz)}{\nu_{reference}\ (MHz)} \qquad (2)$$

As shown above chemical shifts arise due to the nucleus of interest being in a slightly different electronic environment than the reference compound. However additional signals can also arise due to differences in magnetic susceptibilities of substances or compounds.

MAGNETIC SUSCEPTIBILITY

Magnetic susceptibility is a measure of how a sample modifies a magnetic field just as a result of the presence of the sample. When a sample is placed into a magnetic field it becomes magnetized and the sample modifies the field. The magnetization can be considered in terms of two contributions, a bulk macroscopic effect, and a local microscopic effect. The bulk intensity of magnetization is proportional to the magnetic field and the constant of proportionality is known as the bulk susceptibility (χ) of the material. When a substance is placed in a magnetic field it may be drawn to regions of stronger field (paramagnetic) or pushed from regions of stronger field (diamagnetic). Upon closer inspection the magnetic susceptibility can be broken down into two

contributions. The magnetic susceptibility (χ) can be shown to be proportional to the magnetic polarizability (α) and the magnetic moment (μ) of the sample.

$$\chi = (\alpha + \frac{\mu^2}{3kT}) \qquad (3)$$

Most organic compounds have only a negative magnetic polarizability contribution. A negative contribution reduces the effective field on these compounds. Compounds with unpaired electrons have a magnetic moment. For these compounds the magnetic moment is much larger than the polarizability term. Thus χ is positive, and these materials are said to be paramagnetic. Most inorganic and practically all organic compounds are diamagnetic. Strictly speaking the field B_o used in Equation 1 is not the applied field, but the applied field corrected for the effect of bulk magnetization. This correction depends on the sample shape and bulk susceptibility. The magnetic susceptibility correction is usually applied when using an external standard.

Consider a sample mixture consisting of two components namely A and B. Let υ_A and υ_B be the volume fractions of A and B in the sample, and let χ_A and χ_B be the volume susceptibilities of A and B respectively. Volume susceptibility is another term for magnetic susceptibility. Therefore to a first approximation the difference in the volume susceptibility ($\Delta\chi_v$) can be approximated as

$$\Delta\chi_v = \nu_A\chi_A - \nu_B\chi_B \qquad (4)$$

As mentioned earlier bulk magnetic susceptibility correction factors are most often used when an external standard is used. The correction is needed to account for the bulk susceptibility difference between the reference compound and the sample. The normal susceptibility correction is on the order of 0.5 ppm or 50 Hz for protons on a 100 MHz spectrometer. The above analysis is similar to the analysis carried out by Gordon in 1962[30] to explain the solvent splitting in ion-exchange resins.

MAGNETIZATION

Macroscopically, we look at the vector sum of all magnetic dipoles in the sample (see Figure 2). This vector sum, M, called magnetization aligns with B_o at thermal equilibrium and is proportional to the population difference of the two energy states (see Figure 2). By convention the direction of B_o is called the z-axis. In NMR the signal in the xy plane is always detected. To see this signal in FT-NMR (Fourier Transform NMR) the spin system must be modified or perturbed. To perturb the spin system a time-dependent radiofrequency (RF) field B_1, or a pulse, is applied perpendicular to B_o. Now this results in M being flipped away from B_o (z-axis) and can be represented as a longitudinal (z) component (M_z) and a transverse (xy) component (M_{xy}) (see Figure 3).

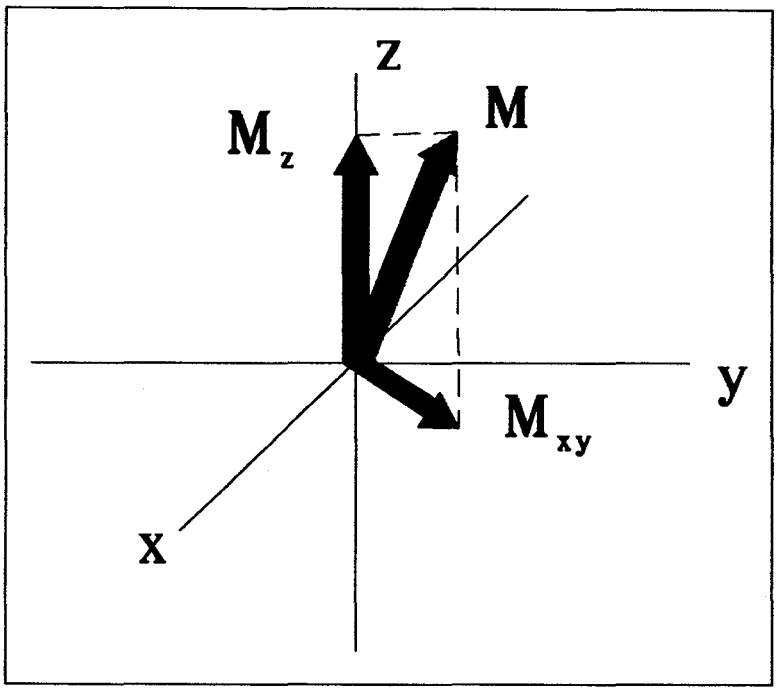

Figure 3. The figure displays how the total magnetization vector can be viewed as an M_z and M_{xy} components.

An NMR signal is detected in the form of an oscillating current induced by M_{xy} through a receiver coil wound about an axis perpendicular to the z-axis or B_o. The signal detected is called a free-induction decay (FID). The time-domain FID is Fourier transformed into a frequency-domain NMR spectrum.

RELAXATION

After a pulse is applied, M can be conveniently visualized as having two components M_z and M_{xy}. These magnetizations then begin to return to equilibrium at a rate usually assumed to be a first-order exponential. These relaxations are called spin-lattice (longitudinal) relaxation and spin-spin (transverse) relaxation for the M_z and M_{xy} components respectively. The time constants for these exponential relaxations are called T_1 for spin-lattice and T_2 for spin-spin relaxation. Spin-lattice relaxation is described by the following equation

$$M_z(t) - M_z(\infty) = (M_z(0) - M_z(\infty)) \exp(-t/T_1) \quad (5)$$

$M_z(t)$ is the magnetization at time t
$M_z(\infty)$ is the magnetization at equilibrium
$M_z(0)$ is the magnetization at t = 0 seconds
t variable delay time
T_1 is the spin-lattice relaxation time constant

Any process which produces a fluctuating magnetic field at the nucleus can result in a relaxation mechanism. The T_1 relaxation mechanisms arise in a number of ways dipole-dipole interactions (dd), quadrupolar interactions (qd), chemical shift anisotropy (csa), scalar coupling (sc), spin rotation interactions (sr) and the presence of paramagnetic species (ps). For nuclei with spin the presence of a fluctuating magnetic field due to the tumbling of nearby magnetic dipoles induces a transition pathway. This type of interaction is called dipole-dipole. For nuclei of spin > 1/2 the presence of the non-symmetric electronic environment induces quadrupolar relaxation. Chemical shift anisotropy arises when the electron density around the nucleus is anisotropic (not evenly distributed). The uneven distribution of electron density causes uneven shielding at the nucleus and thus the magnetic field acting on the nucleus varies with the orientation of the molecule relative to the field. This anisotropy generates a fluctuating field at the nucleus and this can aid in relaxation. In addition scalar coupling relaxation can also aid in relaxation. If chemical exchange is present and the exchange frequency is greater than the frequency of spin coupling, then the exchange process creates a fluctuating field at the site of the exchanging nucleus. A molecular rotation generates a magnetic field which can couple with nuclear spin. This coupling involves a magnetic field at the nucleus and

provides a relaxation mechanism called spin-rotation relaxation. The final mechanism of relaxation to be discussed here is due to the presence of paramagnetic species in the sample. This interaction is normally due to dipolar coupling of the nucleus and the unpaired electrons of the paramagnetic species. In order to determine the mechanisms of relaxation for a particular system, each mechanism must be considered as contributing to the overall relaxation.

As mentioned earlier any process which causes a fluctuating magnetic field can aid in relaxation. For a given system any number of the above mentioned processes maybe present at any time. The relaxation rates due to different mechanisms add together to give the total relaxation in the following manner.

$$T_1^{-1} = T_{1dd}^{-1} + T_{1qd}^{-1} + T_{1csa}^{-1} + T_{1sc}^{-1} + T_{1sr}^{-1} + T_{1ps}^{-1} \qquad (6)$$

The relative contributions of each of these mechanisms to the total relaxation depends on the system. The smaller the value of the T_1 of a particular mechanism the more efficient this mechanism is in causing relaxation. If a selective excitation is used chemical exchange can substantially alter the apparent T_1 of the system .

CHEMICAL EXCHANGE

Chemical exchange is a term that covers both conformational changes and chemical reactions. The following analysis can be used for an exchange between two conformers of a species or two species in equilibrium. Consider for example a two site exchange say sites A and B (see Figure 4).

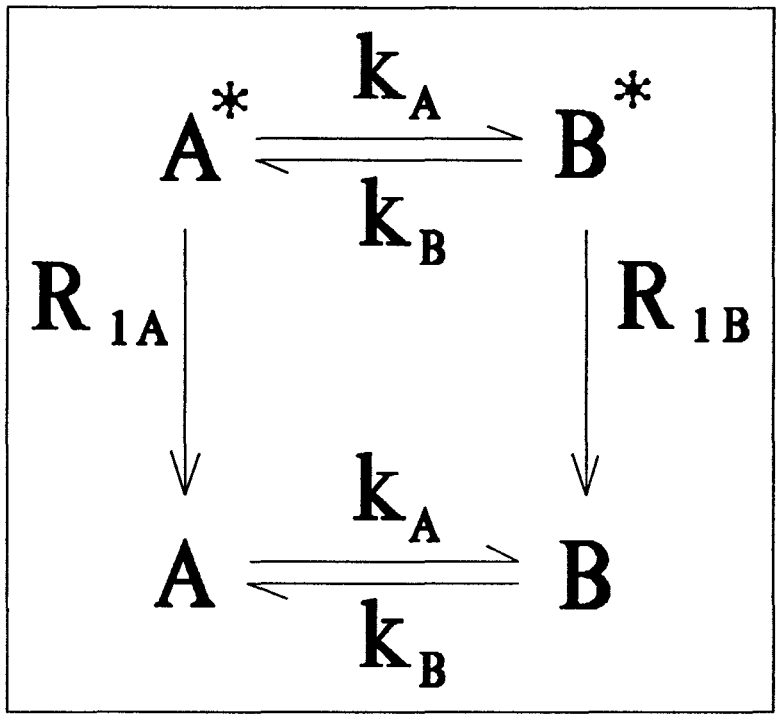

Figure 4. The figure shows schematically the two site exchange/relaxation system.

A^* and B^* represent magnetically perturbed sites A and B.

A and B represent magnetization at equilibrium.

k_A and k_B are the rate constants for exchange from sites A to B and B to A respectively.

R_{1A} and R_{1B} are the relaxation rate constants with no exchange.

R_{1A} and R_{1B} are equal to $1/T_{1A}$ and $1/T_{1B}$ respectively.

The differential equations for the return to equilibrium for sites A and B are

$$\frac{d[M_{zA}(t)-M_{zA}(\infty)]}{dt} = -(1/T_{1A}+k_A)[M_{zA}(0)-M_{zA}(\infty)]+k_B[M_{zB}(0)-M_{zB}(\infty)] \quad (7)$$

and

$$\frac{d[M_{zB}(t)-M_{zB}(\infty)]}{dt} = +k_A[M_{zA}(0)-M_{zA}(\infty)]-(1/T_{1B}+k_B)[M_{zB}(0)-M_{zB}(\infty)] \quad (8)$$

respectively.

$M_{zA}(t)$, $M_{zB}(t)$ represent the magnetizations at any time t of sites A and B respectively immediately after a perturbation.

$M_{zA}(\infty)$, $M_{zB}(\infty)$ represent the equilibrium magnetization of A and B respectively. The values of T_{1A}, T_{1B}, k_A, and k_B can be determined readily by conducting inversion recovery experiments. There are two types of inversion recovery experiments which can be used, namely nonselective and selective inversion recovery. These two types of experiments are designed to measure different aspect of the relaxation process.

First consider the non-selective inversion recovery experiment for a two site exchange system as described above. For a non-selective inversion recovery experiments common the pulse sequence used is 180° - τ - 90°. When the 180° pulse is applied the magnetization that was along +z is flipped down to -z. For a spin-lattice relaxation process this magnetization will relax back along z to equilibrium at a rate determined by the $1/T_1$'s and k's of the system. The initial magnetization of site A and B will be $M_{zA}(0)$ and $M_{zB}(0)$ respectively, and the equilibrium magnetization for A and B will be $M_{zA}(\infty)$ and $M_{zB}(\infty)$ respectively. If the inversion recovery pulse is exactly 180° then the initial

conditions of the relaxation are $M_{zA}(0) = -M_{zA}(\infty)$ and $M_{zB}(0) = -M_{zB}(\infty)$. Using equations 7 and 8 and the above conditions the relaxation equation for site A is

$$\frac{d[M_{zA}(t)-M_{zA}(\infty)]}{dt} = -(1/T_{1A}+k_A)[2M_{zA}(0)]+k_B[2M_{zB}(0)] \quad \textbf{(9)}$$

and similarly for site B. Actually in a T_1 experiment a series of measurements are conducted by using a variable delay (τ) between the 180° inversion pulse and the 90° detection pulse. This 180° - τ - 90° pulse sequence can be used for any number of exchanging sites.

For a selective inversion recovery experiment the initial conditions are different. Again consider a two site exchange system, where A is inverted and B is not inverted. The initial conditions for A and B are then $M_{zA}(0) = -M_{zA}(\infty)$ and $M_{zB}(0) = M_{zB}(\infty)$ respectively. Again using equations 1 and 2 and the above conditions, the relaxation equations for site A and B then becomes

$$\frac{d[M_{zA}(t)-M_{zA}(\infty)]}{dt} = -(1/T_{1A}+k_A)[2M_{zA}(0)]+k_B[(0)] \quad \textbf{(10)}$$

and

$$\frac{d[M_{zB}(t)-M_{zB}(\infty)]}{dt} = +k_A[2M_{zA}(0)]-(1/T_{1B}+k_B)[(0)] \quad \textbf{(11)}$$

A similar situation would exist for a selective inversion on site B. A common pulse sequence for a selective inversion recovery is 90° - τ - 90° - τ_2 - 90°.

The selective inversion pulse sequence is the same as the non-selective pulse

sequence except the 180° pulse in the non-selective sequence is replaced by a 90° - τ - 90° in the selective inversion recovery sequence. The 90° - τ - 90° is convenient to set-up the selective inversion condition. Figure 5 helps to illustrate a two site selective inversion experiment. The transmitter frequency is set equal to the frequency of the signal to be inverted. A delay between the 90° pulse is equal to $1/2\Delta\nu$ where $\Delta\nu$ is the frequency difference between the two signals. This delay allows the signals to get 180° out of phase as shown in Figure 5c. A modification in this sequence was needed for this analysis and this will be discussed later in the results section. The constants T_{1A}, T_{1B}, k_A and k_B can be determined by selective and non-selective inversion recovery experiments. A multi-site exchange fitting program SIFIT by Muhandiram and McClung[41] was used to fit the experimental data.

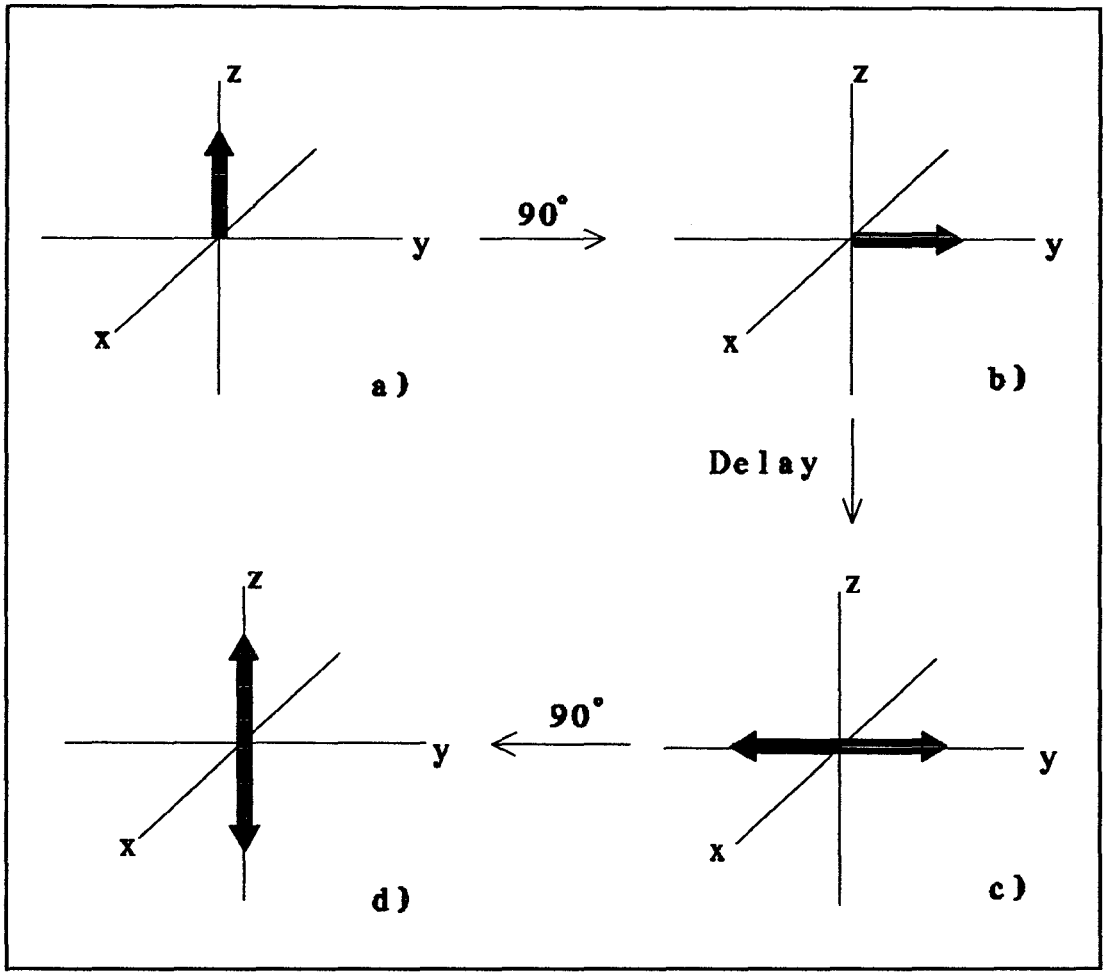

Figure 5. The figure shows the magnetization vector representation of a selective inversion recovery experiment.

LINEWIDTHS

In analyzing linewidths there are two quite different types of broadening, coherent and incoherent line broadening. These two types of broadening are also known as homogenous (incoherent) broadening and inhomogeneous (coherent) broadening. The type of broadening due to a superposition of many different sharp signals is called coherent line broadening. In contrast incoherent line broadening can simply be defined as the types of broadening that are not due to a distribution of sites. There are many

sources of incoherent linebroadening, namely chemical shift anisotropy and dipolar broadening. From the linewidths of a peak an estimate of T_2 can be determined.[7] The linewidths at halfheight ($\Delta\nu_{1/2}$) are inversely proportional to T_2.

$$\Delta\nu = 1/\pi T_2^* \qquad (12)$$

Where T_2^* is the effective spin-spin lattice relaxation time constant. The other sources of incoherent line broadening are slow motion and chemical exchange.

TEMPERATURE

Temperature dependent phenomena may provide information about the solvent-polymer interactions. The main reason for varying the temperature is to see if chemical exchange between the two sites may be occurring. There are two features in the spectra that may change if a temperature dependent process is present. The frequency difference between the two sites may change and their linewidths may also change. If the two sites are in chemical exchange, one would expect that the signals may come closer together. The linewidths of an exchanging system may broaden the peaks. If no change in chemical shift difference or change in linewidths is observed, this will only indicate that the exchange process is not sensitive over the temperature range analyzed. There have only been a couple of studies that have specifically looked for a temperature dependence on the solvent splitting.[31,34]

In cationic ion-exchange resins (DOWEX-50) Creekmore and Reiley[34] observed a temperature dependence on the chemical shift between the internal and external water peaks. They noted that for sodium and magnesium counter-ions of 8% cross-linked polystyrene divinylbenzene that as the temperature (5°C to 70°C) increased, the two peaks

moved apart. As mentioned earlier if the two sites were in chemical exchange one would expect the signals to move closer as the temperature was increased. In addition it was shown that for the sodium counter-ion resins that the chemical shift difference increased with increase of the percent cross-linking (2% to 12%).

In a carboxylic acid[42] resin with a polymer backbone described as a cross-linked acrylic, the temperature effect on the chemical shift difference and the linewidths of the interior and exterior peaks were studied. It was speculated that the probable cause of the chemical shift and linewidth effect was due to an interaction between the carboxylic acid group and water. However the author admitted that the details of this interaction are still obscure.

Ford *et al*[31] studied toluene splitting in cross-linked polystyrene gel beads 16-18% ring substituted with benzyltri-n-butylphosphonium chloride groups. A sample of 2% cross-linked polymer in toluene was studied from -31°C to 74°C. Over this temperature range no apparent trend in the linewidth of the external methyl peak was observed. The exterior methyl peak linewidth could not be determined. There was no apparent chemical shift difference dependence on temperature. In addition the apparent T_1's of the exterior and interior methyl peaks increased as the temperature increased from +1°C to 74°C and became nearly equal at 74°C. The T_1 of the exterior methyl peak is always greater than interior methyl peak. The values of the T_1's of toluene inside and outside with the polymer present were always smaller than the T_1's of neat toluene. This reduction in all the T_1's suggests that the toluene motion is slower in the polymer sample than that of toluene in solution. Ford *et al*[31] were not able to fully determine the T_1 mechanisms.

mechanisms.

SWELLING MEASUREMENTS

Swelling phenomena can be quantified based on thermodynamic considerations. The change in the Gibbs free energy of mixing (ΔG_m) of the solvent and the polymer is usually considered. Let the free energies of the pure solvent, the free energy of the pure polymer and the free energy of the solvent-polymer system be represented G_1, G_2 and G_{12} respectively.

$$\Delta G_m = G_{12} - G_2 - G_1 \qquad (13)$$

It can be shown[43] that the free energy of mixing can be expressed as shown below.

$$\Delta G_m = kT(n_1 \ln v_1 + n_2 \ln v_2 + X n_1 v_2) \qquad (14)$$

k Boltzmann's constant
T Temperature (K)
n_1 number of solvent molecules
n_2 number of polymer molecules
v_1 volume fraction of solvent in the solution
v_2 volume fraction of polymer in the solution
X the solvent-polymer interaction parameter

X is a dimensionless quantity which characterizes the interaction energy per solvent molecule divided by kT. Alternatively the quantity kTX represents the difference in energy of a solvent molecule immersed in almost pure polymer compared with solvent in pure solvent. The chemical potential of the solvent (μ_1) in the solution relative to its

free energy of mixing (ΔG_m) with respect to the number of solvent molecules at constant temperature and pressure.

$$\mu_1 - \mu_1^o = \left(\frac{\partial(\Delta G_m)}{\partial n_1}\right)_{n_2,T,P.} \tag{15}$$

where

$$\left(\frac{\partial(\Delta G_m)}{\partial n_1}\right)_{n_2,T,P.} = RT[\ln(1-v_2) + (1-1/x)v_2 + Xv_2^2] \tag{16}$$

x is the ratio of the molar volumes of solvent v_1 and the molar volume of the polymer v_2 ($x = v_2/v_1$). The above equation is usually written in the form below:

$$\mu_1 - \mu_1^o = RT[\ln(1-v_{2m}) + \chi v_{2m}^2 + v_{2m}] \tag{17}$$

Where v_{2m} is the volume fraction of the polymer at equilibrium (maximum) swelling. Although in this study neither X nor v_{2m} will be determined, the increase in swelling by volume of the polymer was sufficient in this study to measure the swelling characteristics of the polymer system.

As mentioned earlier for cross-linked polymer systems one can obtain a measure of the extent of branching of the polymer network by conducting swelling measurements. The swelling measurements involve measuring the size increase of the polymer before and after the addition of solvent. The amount of swelling that occurs depends on the relative amount of cross-linker present and on the solvent used. Generally, as the weight percent

of the cross-linker increases the swelling decreases. For a given percent of cross-linker different solvents will show different swelling. The ability of solvents to cause the polymer to swell depends on how the solvent and polymer interact. After the synthesis of cross-linked polymers, it is hard to measure directly the amount of cross-linker present and the amount of unreacted double bonds. The swelling measurement allows one to characterize polymers without any assumptions about the amount of cross-linker present. Swelling measurements thus provide a measure of the rigidity of the polymer network.

NMR can provide many ways of analyzing solvent-polymer interactions. The origin of the solvent splitting has been explained to a first approximation by Gordon in 1962. The plausibility of magnetic susceptibility in causing the solvent splitting will be analyzed. An attempt will be made to characterize the polymer by calculating their exchange rates. Parameters like linewidths, peak areas, chemical shift difference, and swelling ability will be measured. In addition isotope and temperature effects will be analyzed to try to establish the type of interaction.

Chapter 3

RESULTS

Previous studies on the solvent splitting of swollen EGDMA/MMA polymer in chloroform have focused on the exchange rates of $CDCl_3$ as a function of weight percent cross-linker.[29] It was hoped that through analyzing many solvent-polymer systems a mechanism could be established for the solvent-polymer splitting. The experiments involved measuring the increased swelling by volume, the chemical shift difference and the linewidths for various weight percent EGDMA in EGDMA/MMA polymer and solvents. In addition variable temperature studies were conducted to determine the temperature effect on the linewidths and the chemical shift difference.

SYNTHESIS of EGDMA/MMA Polymer

The cross-linked EGDMA/MMA polymer system was synthesized using a free radical bulk polymerization process. Known weights of EGDMA, MMA and the free radical initiator (AIBN azobisisobutyronitrile) were placed in a round-bottom flask. The flask was then placed in a water bath for 24 hours at 70°C. The total starting weight of the polymer varied between 5-10 grams. An expandable rubber fitting was placed on the flask, to allow an easy means of release of the nitrogen evolution during polymerization. After the reaction was completed the polymer was swollen in methylene chloride to form a gel (usually 1-2 hours). The gel was then filtered using a Büchner filter funnel. The

polymer was washed first with 50ml methanol, then with 100ml methylene chloride, and the wash cycle was repeated once. The polymers usually swell 2-10 times its size, depending on percentage cross-linker, in methylene chloride and it collapses when placed in methanol. The methylene chloride swollen polymer was placed into a soxhlet to extract impurities. Upon removal from the soxhlet, the polymer was washed with methanol and then left to dry. The weight percent of EGDMA in EGDMA/MMA polymer synthesized was 0.7, 2.1, 3.3, 4.8, 9.2 and 16.5.

CHARACTERIZATION OF SPLITTING

The solvent splitting for EGDMA/MMA polymer was first noted in chloroform.[29] If the solvent-polymer interaction is actually a chemical bonding between the two, an isotope dependence may exist for $CHCl_3$ and $CDCl_3$. The ^1H and ^2H splitting was observed at 500 MHz and 76.8 MHz respectively. In order to determine if an isotope effect exists one can compare the peak areas, the frequency difference and the linewidths of the two signals for each of isotopomers.

The chemical shift difference ($\Delta\delta_{ps}$) is defined as the chemical shift of the solvent associated with the polymer (δ_p) minus the chemical shift of the solvent not associated with the polymer(δ_s). The two types of solvents will be referred to as bound solvent for solvent associated with the polymer and free solvent for solvents not associated with the polymer.

$$\Delta\delta_{ps} = \delta_p - \delta_s \qquad (18)$$

A positive $\Delta\delta_{ps}$ indicates that the bound solvent is less shielded by electrons than the free solvent. This definition may differ from chemical shift difference in the literature as some authors define the chemical shift difference as the solvent chemical shift minus the polymer chemical shift. The above definition will be used from now on in this document.

The bound solvent and free solvent peaks were identified in the spectrum in the following manner. The polymer was placed in a nmr tube and swollen in an excess of solvent. The method was varying the amount of polymer present in the detection range of the probe on the spectrometer, and the observing the corresponding spectra. As more polymer was present in the detection area of the probe, the greater the relative amount of bound solvent in the spectra. The height of the polymer present in the probe was varied by using a vortex plug in the sample. For a majority of solvent used the polymer floated in the solvent. All of the bound and free solvents were identified in this manner.

Nucleus	$\Delta\nu$ (Hz)	$\Delta\delta_{ps}$	Ratios of areas (free/bound)	Linewidths	
				bound	free
Deuterium	11.7	0.152	1.10	1.9	1.7
Proton	75.8	0.150	1.04	13.7	20.8

Table 2. The frequency difference ($\Delta\nu$), the chemical shift difference ($\Delta\delta_{ps}$), the ratio of peak area, and linewidths for the free and bound solvents in the ^{1}H and ^{2}H are displayed for 2 weight percent EGDMA/MMA polymer. All peaks fitted to Lorentzian absorption lineshapes, and linewidths were taken at half peak height.

If there is a preference for one of the isotopomers of chloroform to interact with the polymer, an analysis of the peak areas may illustrate this. For ^{1}H and ^{2}H two signals were present for each type of chloroform solvent, one for the bound solvent and one for

the free solvent. These peaks were identified for each nucleus as discussed above. The ratios of the peak areas for ^1H and ^2H are 1.04 and 1.10 respectively (see Table 2). The ratios do not differ significantly enough to show an isotope preference. Thus no isotope dependence has been observed based on analyzing the peak areas.

Another way of indicating an isotope dependence is to observe a frequency difference between the free and bound solvent of the two isotopomers. In order to analyze the frequency splitting, one must consider what splitting is expected for ^2H when ^1H is split by a certain amount. If no isotope effect is present, the expected frequency splitting is related to the magnetogyric ratios $\gamma_H/\gamma_D = 6.51$ (See Table 1.). Therefore the frequency splitting for ^1H should be 6.51 times that for ^2H. The frequency difference for ^1H was 76.6 Hz, and therefore the expected frequency splitting for deuterium $\Delta\nu(^2H)$ should be 11.6 Hz, relative to proton splitting $\Delta\nu$ (^1H) observed.

$$\Delta\nu(^2H) = \Delta\nu(^1H)\left(\frac{\gamma_D}{\gamma_H}\right) = (75.8)(1/6.51)=11.6\ Hz \qquad \textbf{(19)}$$

The $\Delta\nu(^2H)$ calculated is in agreement with the experimental value in Table 2, therefore no isotope effect seems to be present.

The analysis of peak areas and frequency difference indicates that no isotope dependence exists. As mentioned earlier the linewidths, may also indicate an isotope effect, however an analysis of linewidths is difficult due to the many different mechanisms of linebroadening. Table 2 shows how the linewidths for the protons signals are greater than those for the deuterium signals. Although no isotope effect is observed

the solvent-polymer interaction may be sensitive to temperature.

TEMPERATURE STUDIES

The sample chosen for the temperature study was a sample of 2 weight percent EGDMA in EGDMA/MMA polymer in 20 weight percent $CHCl_3$ and 80 weight percent $CDCl_3$. Five temperatures were analyzed over a temperature range of -30°C to 45°C. The spectrum at 0°C is shown in Figure 6. The proton coupled ^{13}C spectra was acquired using a 90° - Acquire - Delay with a delay of $5T_1$ ($T_1(CDCl_3)$=70 s) and spectrometer frequency of 62.87 MHz. The normal proton coupled ^{13}C spectra containing $CHCl_3$ and $CDCl_3$ should contain 5 resonances, two due to $CHCl_3$ (^1H has spin=1/2) and three due to $CDCl_3$ (^2H has spin=1). The $CHCl_3$ and $CDCl_3$ resonances are separated by J_{CH} = 210 Hz and by J_{CD} = 32 Hz respectively. When the gel is present all the signals split as shown in the spectrum at 0°C. Table 3 summarizes the data over the temperature range analyzed.

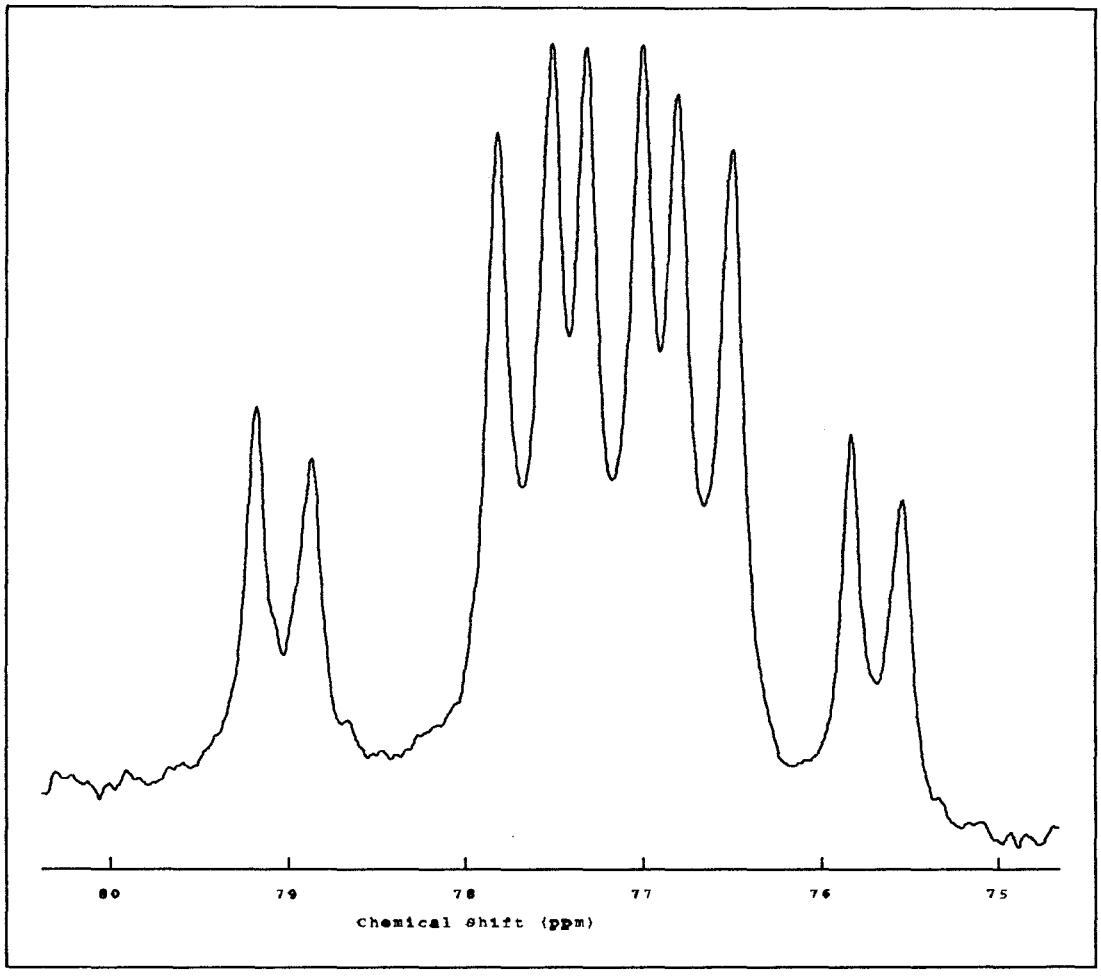

Figure 6. The spectrum displayed above is the ^{13}C proton coupled spectrum of chloroform (20 weight percent $CHCl_3$ / 80 weight percent $CDCl_3$) at 0°C in 2 weight percent EGDMA/MMA polymer.

Temperature	Area Ratios		Δν(Hz)	
	$CHCl_3$	$CDCl_3$	$CHCl_3$	$CDCl_3$
-30°C	1.29	1.43	19.2	19.3
-17°C	1.08	1.25	18.9	19.2
0°C	1.0	0.90	18.5	18.8
25°C	1.0	0.80	18.5	19.1
45°C	1.0	0.90	18.5	18.5

Table 3. The ^{13}C peak area ratios and frequency difference (Δν) for the free and bound solvents for chloroform in 2 weight percent EGDMA in EGDMA/MMA polymer as a function of temperature. The peak area ratios are the bound peak areas divided by that of the free solvent, and each line of each spectrum was fitted to a Lorentzian lineshape. The temperatures reported varied $\pm$2°C from the values stated in Table 3.

The estimate of the errors in the area ratios, the Δν difference and the linewidths are about 5%, thus all the values in Table 3 are essentially within experimental error. Although no temperature or isotope effects have been observed for the solvent-polymer system analyzed, the swelling measurements are very sensitive to the solvent-polymer systems analyzed.

SWELLING MEASUREMENTS AND CHEMICAL SHIFT DIFFERENCE

In the early stages of this analysis, it was speculated that the splitting maybe caused solely by a physical interaction between the polymer and the solvent. Thus, in addition to measuring the chemical shift differences as a function of percent cross-linker and solvent, the swelling increase of the polymer was also measured. The swelling measurements were conducted in 5mm NMR tubes. Typical analysis involves placing the polymer in the tube, with an appropriate amount of the solvent. The sample was usually left for 1 day and the percent increase in the height of the sample was measured.

Swelling measurements as a function of weight percent EGDMA/MMA polymer cross-linked polymer in $CHCl_3$ is shown in Table 4. All the swelling measurements are based on the percent increase in height of the swollen polymer relative to the dry polymer.

Weight Percent EGDMA/MMA polymer	Swelling Percent Increase	Chemical Shift Difference ($\Delta\delta_{ps}$) ^{13}C	Chemical Shift Difference ($\Delta\delta_{ps}$) ^{1}H
0.7	460	0.120	0.032
2.1	380	0.189	0.051
3.3	265	0.270	0.075
4.8	220	0.314	0.084
9.2	170	0.415	0.104

Table 4. The swelling percent increase of the EGDMA/MMA polymer system, and the ^{13}C and ^{1}H chemical shift difference ($\Delta\delta_{ps}$) for chloroform as a function of weight percent EGDMA in EGDMA/MMA polymer. The swelling measurements increase measurements were done in duplicate and the error of the measurements is about 10%.

Table 4 shows clearly how sensitive the swelling measurements are to the weight percent of cross-linker present. In the lowest percent cross-linker (0.7 wt% EGDMA) an increase in volume of five times was observed. The effect of the amount of cross-linking on the swelling decreases substantially over the region analyzed. Although for the highest percent cross-linking network, the swelling only doubled in size, but this swelling was still quite noticeable. Table 4 also shows the ^{13}C and ^{1}H chemical shift difference between the two sites as a function of cross-linking. Table 4 displays that as the weight percent of cross-linker increases the chemical shift difference increases. As will be shown later, this trend was the same for all the solvent-polymer systems that were analyzed as

a function of weight percent cross-linker. As mentioned earlier the swelling measurements are an indicator of the rigidity of the polymer. From Table 4 one can see that the as the swelling increases the chemical shift difference increases. Figure 9 shows an almost linear dependence of the chemical shift difference on the swelling. The value of the slope from the plot of the swelling percent increase against ^{13}C chemical shift difference is about 0.001 chemical shift difference per percent swelling increase (ppm/%). A similar trend of increasing chemical shift difference with increasing percent cross-linker is observed. For the protons, the dependence of the swelling on the chemical shift difference is about 0.00025 ppm/%. Not only was the swelling increase and chemical shift difference measured for EGDMA/MMA polymer in chloroform, but also in methylene chloride.

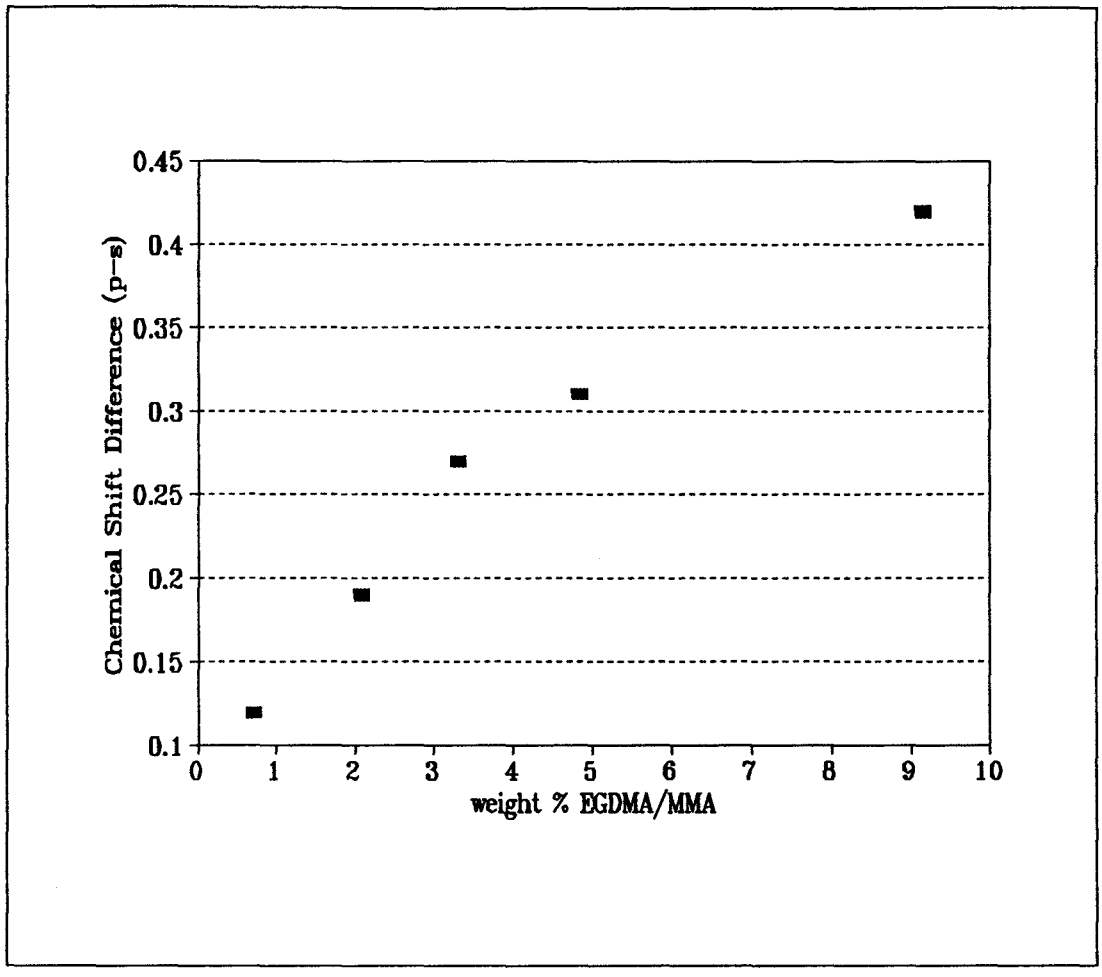

Figure 7. The graph displays the ^{13}C chemical shift difference ($\Delta\delta_{ps}$) of chloroform versus the weight percent of cross-linker (EGDMA) in EGDMA/MMA polymer.

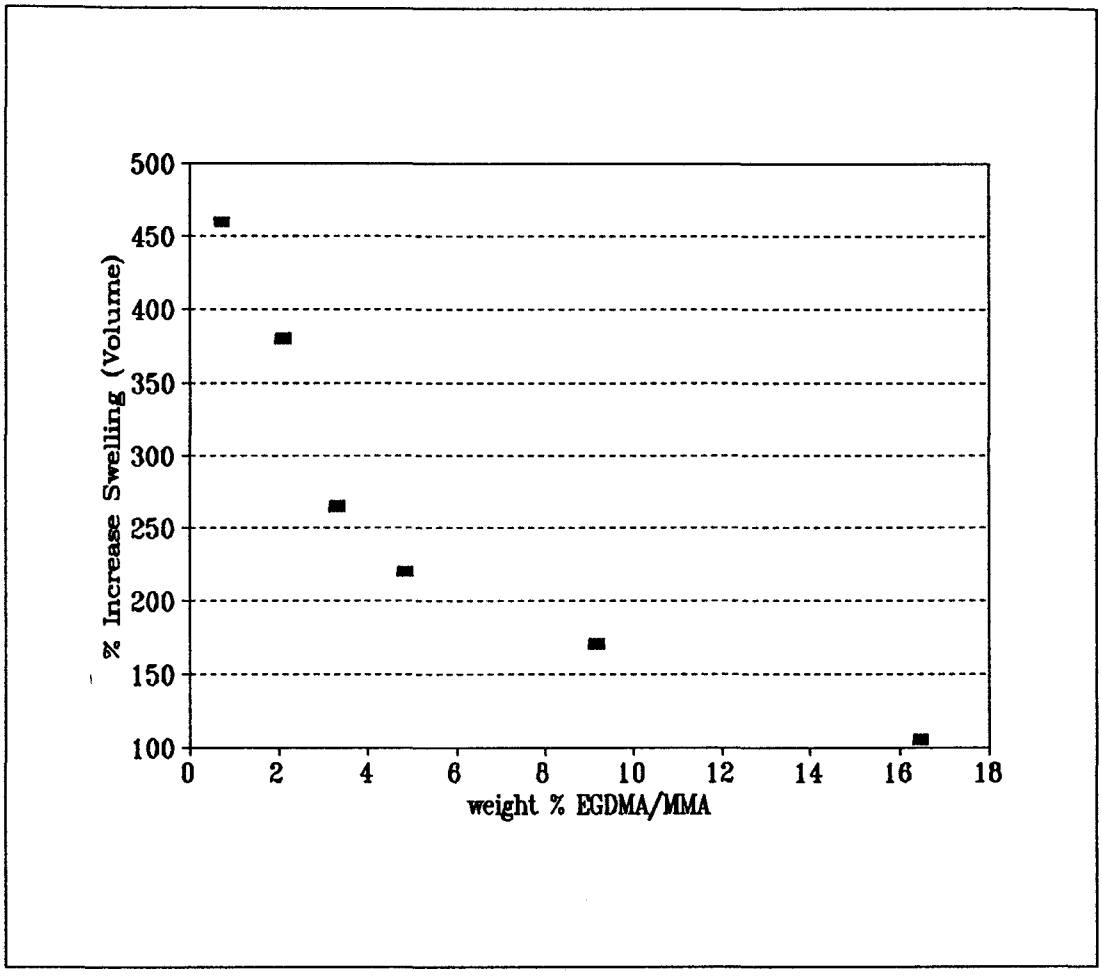

Figure 8. The graph displays the increase in swelling percentage of the polymer versus the weight percent cross-linker EGDMA in EGDMA/MMA polymer in chloroform.

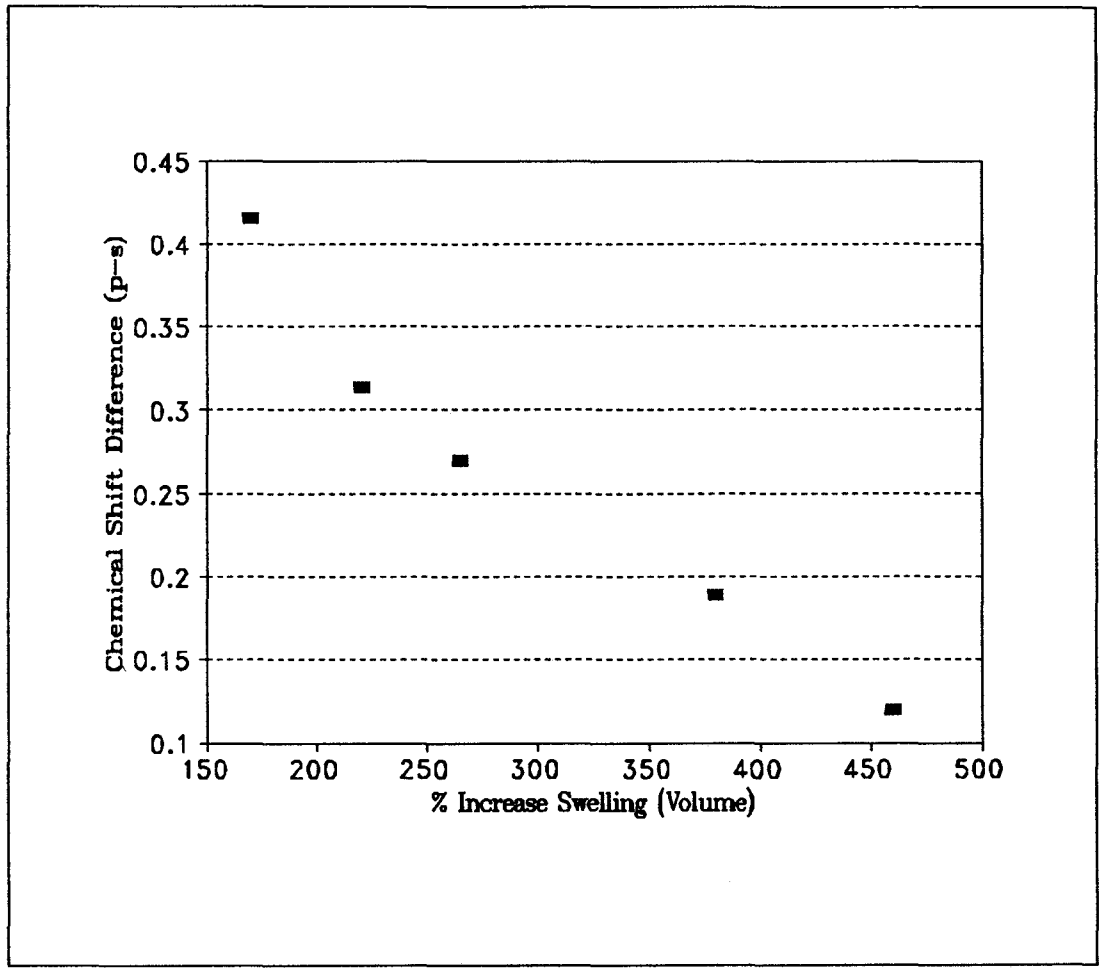

Figure 9. The graph displays the ^{13}C chemical shift difference of chloroform versus the increase in swelling percentage of the polymer.

Table 5 summarizes the swelling measurements, chemical shift differences for carbon and proton for various cross-linking in methylene chloride.

Weight Percent EGDMA/MMA polymer	Swelling Percent Increase	Chemical Shift Difference ($\Delta\delta_{ps}$) ^{13}C	Chemical Shift Difference ($\Delta\delta_{ps}$) ^{1}H
2.1	340	0.070	0.051
3.3	300	0.083	0.066
4.8	210	0.110	0.071
9.2	170	0.166	0.104
16.5	120	0.216	0.127

Table 5. The swelling percent increase of the EGDMA/MMA polymer system, and the ^{13}C and ^{1}H chemical shift difference ($\Delta\delta_{ps}$) for methylene chloride as a function of weight percent EGDMA in EGDMA/MMA polymer.

The data for methylene chloride shows trends similar to that for chloroform. The dependence of the chemical shift difference as a function of the swelling of the polymer shows a linear behaviour. The corresponding slopes for chloroform (0.001 ppm/% (^{13}C), 0.00025 ppm/% (^{1}H)) differ from those of methylene chloride (0.00067 ppm/% (^{13}C), 0.00033 ppm/% (^{1}H)). For a given weight percent EGDMA in EGDMA/MMA polymer the ^{13}C chemical shift difference in chloroform is 2/3 the value of the ^{13}C chemical shift difference in methylene chloride, and the ^{1}H chemical shift difference in chloroform is 4/3 the value of the ^{1}H chemical shift difference in methylene chloride.

In addition to measuring the swelling increase and the chemical shift difference as a function of weight percent EGDMA/MMA polymer for chloroform and methylene chloride similar studies were conducted on bromobenzene, chlorobenzene, iodobenzene, and aniline solvent systems. The swelling measurements as a function of weight percent

EGDMA in EGDMA/MMA polymer for these solvents are shown in Table 6.

Weight Percent EGDMA/MMA polymer	Increase Percent Swelling			
	bromo-benzene	chloro-benzene	iodo-benzene	aniline
0.71	120	160	240	415
2.08	92	115	80	245
3.30	91	110	10	210
4.83	80	75	10	155
9.16	21	0	10	50
16.47	17	0	5	47

Table 6. The swelling percent increase of the EGDMA/MMA polymer system for bromobenzene, chlorobenzene, iodobenzene and aniline as a function of weight percent EGDMA in EGDMA/MMA polymer.

For each of the solvents analyzed the swelling decreases as the weight percentage of cross-linker increases. In the case of chlorobenzene for higher weight percent polymer the solvent is not able to cause any detectable swelling increase. For each of these four solvents only the carbon spectra were analyzed. This does not mean that splitting would not occur in the proton spectrum but the spectrum was too complex to analyze properly. Three of these four substituted aromatic solvents displayed splitting in the carbon spectrum. Bromobenzene, chlorobenzene, and aniline showed splittings at both 50 MHz and 125 MHz. Iodobenzene did not show any splitting even at 125 MHz over the full range of the weight percent EGDMA in EGDMA/MMA polymer analyzed. Bromobenzene, chlorobenzene and aniline showed splitting for weight percent cross-linking 1 to 5%. The splitting for a given weight percent of cross-linker also differed for

a given solvent depending where the carbon is positioned on the phenyl ring. The next three tables list the chemical shift difference as a function of percent cross-linker, solvent and position on the phenyl ring.

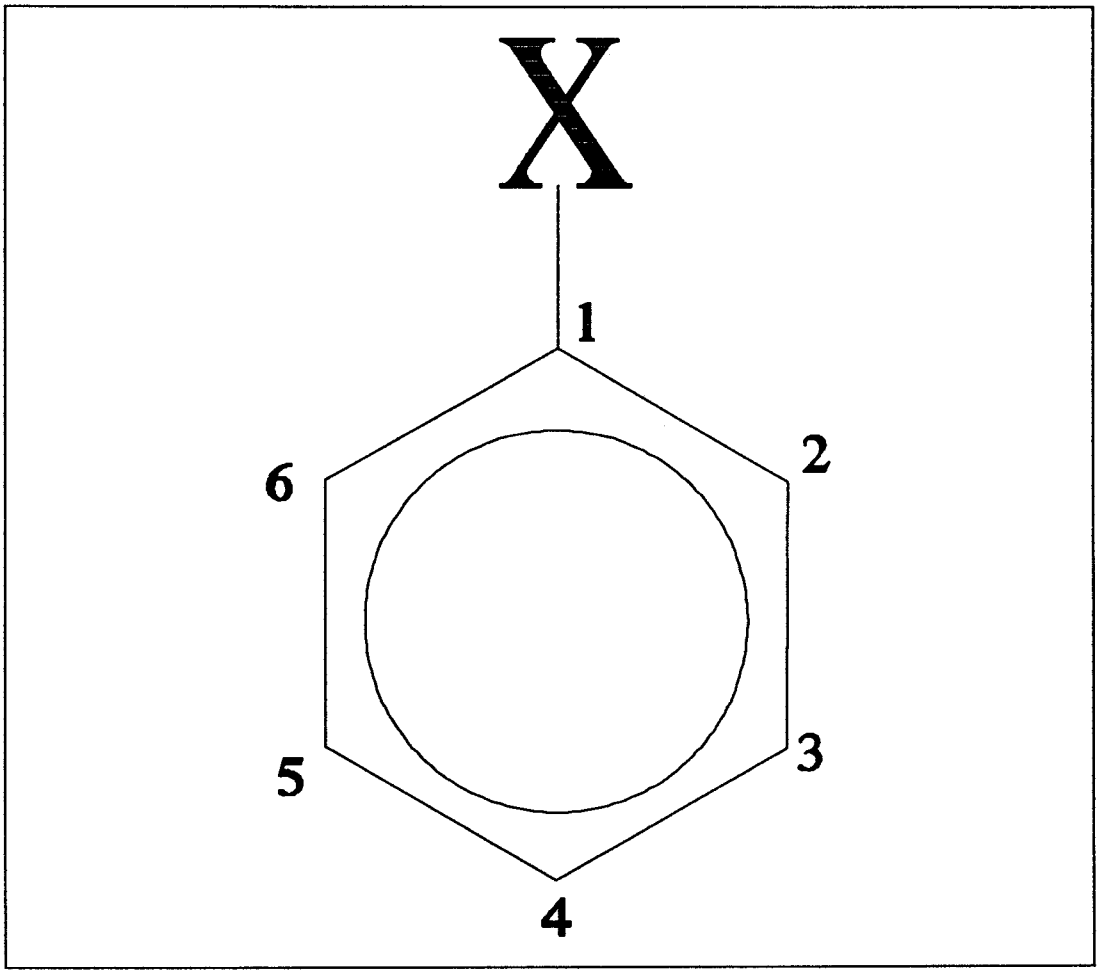

Figure 10. The **X** in the above diagram marks the position of the heteroatom. The numbering of the carbons is displayed, and this numbering will be used in the rest of the text.

Weight Percent EGDMA/MMA polymer	Chemical Shift Difference ($\Delta\delta_{ps}$)			
	C1	C2/6	C3	C4
0.7	0.081	-0.066	NS	-0.095
2.1	0.102	-0.066	NS	-0.098
3.3	0.145	-0.068	NS	-0.125
4.8	0.172	-0.078	NS	-0.147
9.2	NS	NS	NS	NS
16.5	NS	NS	NS	NS

Table 7. The ^{13}C chemical shift difference ($\Delta\delta_{ps}$) for aniline as a function of weight percent EGDMA in EGDMA/MMA polymer. NS means that the signals were Not Split.

Weight Percent EGDMA/MMA polymer	Chemical Shift Difference ($\Delta\delta_{ps}$)			
	C1	C2/6	C3/5	C4
0.7	NS	0.038	0.104	0.102
2.1	NS	0.059	0.148	0.147
3.3	NS	0.078	0.207	0.203
4.8	NS	0.102	0.237	0.235
9.2	NS	NS	NS	NS
16.5	NS	NS	NS	NS

Table 8. The ^{13}C chemical shift difference ($\Delta\delta_{ps}$) for chlorobenzene as a function of weight percent EGDMA in EGDMA/MMA polymer. NS means that the signals were Not Split.

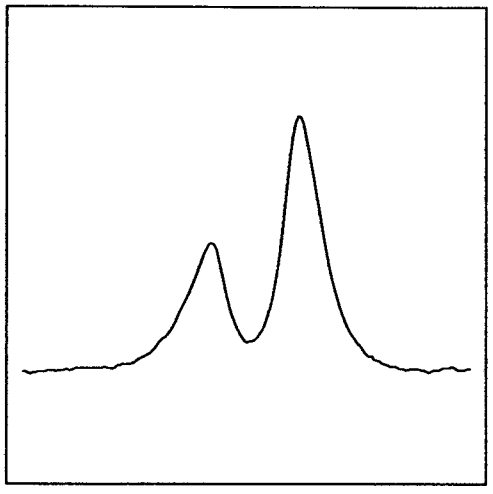

Figure 11. Carbon #1

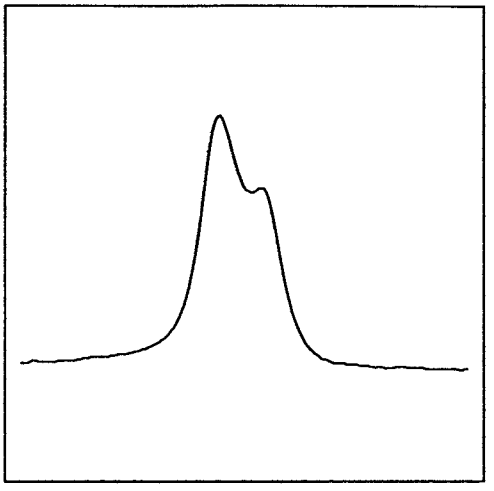

Figure 12. Carbons #2 and #6

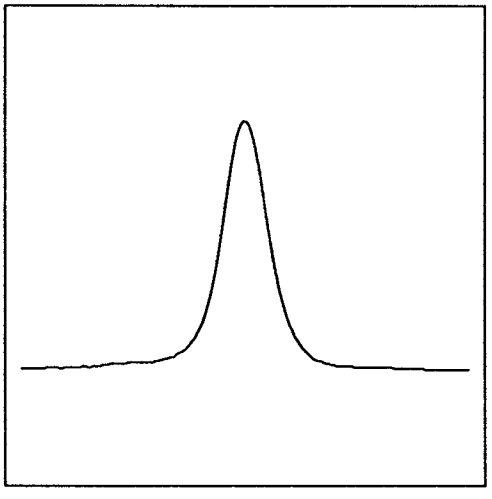

Figure 13. Carbons #3 and #5

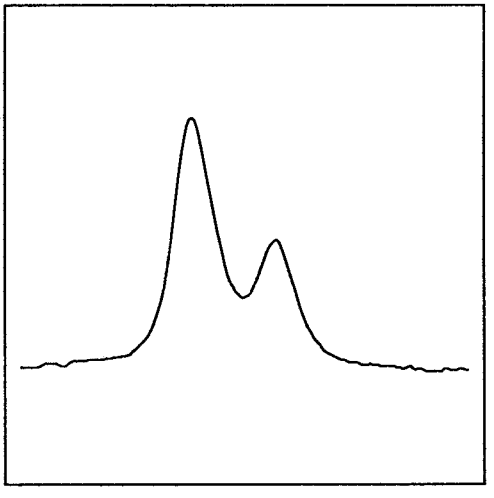

Figure 14. Carbon #4

The above figure displays the solvent splitting for aniline in 4.8 weight percent EGDMA in EGDMA/MMA polymer at 125 MHz. The ^{13}C spectra shown are for the four carbon resonances. The frequency displayed in all 4 figures is 100 Hz (0.8ppm).

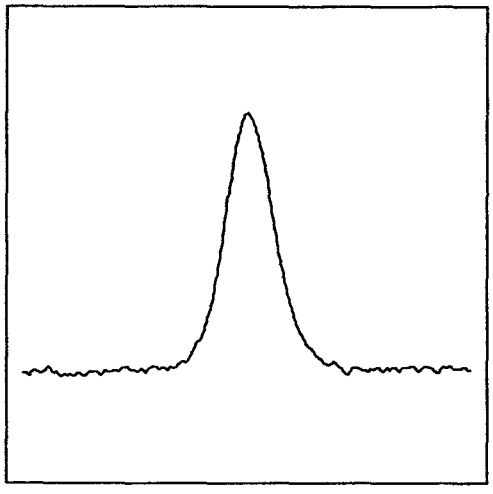

Figure 15. Carbon #1

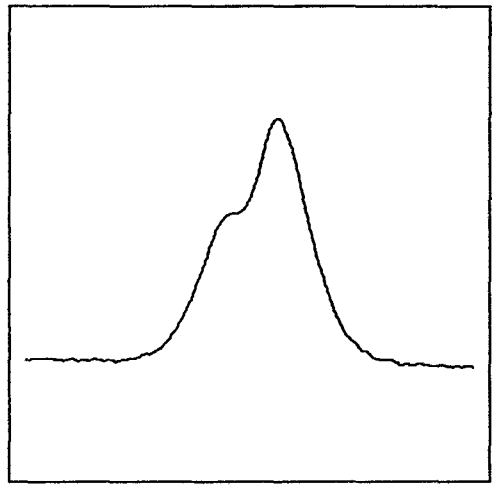

Figure 16. Carbons #2 & #6

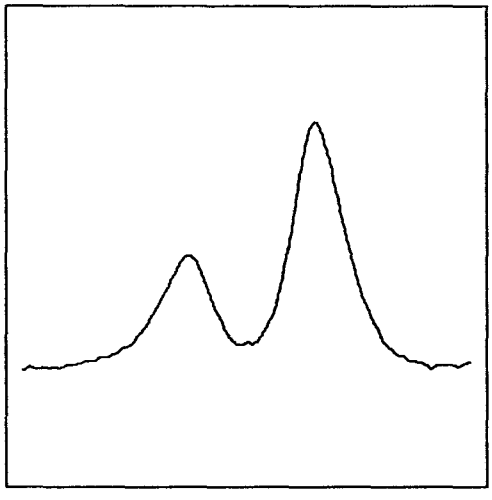

Figure 17. Carbons #3 & #5

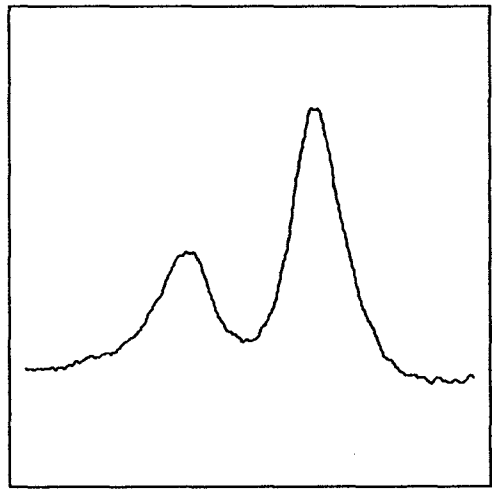

Figure 18. Carbon #4

The above figure displays the solvent splitting for chlorobenzene in 4.8 weight percent EGDMA in EGDMA/MMA polymer at 125 MHz. The ^{13}C spectra shown are for the four carbon resonances on the ring. The frequency range displayed in all 4 figures is 100 Hz (0.8ppm).

Weight Percent EGDMA/MMA polymer	Chemical Shift Difference ($\Delta\delta_{ps}$)			
	C1	C2/6	C3/5	C4
0.7	NS	0.046	0.104	0.097
2.1	NS	0.056	0.148	0.147
3.3	NS	0.058	0.207	0.203
4.8	NS	0.093	0.237	0.235
9.2	NS	NS	NS	NS
16.5	NS	NS	NS	NS

Table 9. The ^{13}C chemical shift difference ($\Delta\delta_{ps}$) for bromobenzene as a function of weight percent EGDMA in EGDMA/MMA polymer. NS means that the signals were Not Split.

The chemical shift difference for chlorobenzene and bromobenzene showed similar behaviour. All chemical shift differences ($\Delta\delta_{ps}$) were found to be positive. The splitting for chlorobenzene and bromobenzene was observed for the ortho, meta and para carbons. The splitting was the same for the meta and para carbons in both chlorobenzene and bromobenzene. The ortho splitting is about half that of the meta and para splitting in both solvents. The chemical shift difference increases with increasing weight percent EGDMA in EGDMA/MMA polymer. The splitting for aniline differs greatly than that of chlorobenzene and bromobenzene in a number of ways. For chlorobenzene and bromobenzene the splitting was observed at the ortho, meta and para carbons, while in aniline the ipso, ortho and para carbons split. The splitting increased as the weight percent EGDMA in EGDMA/MMA polymer increase. Although the $\Delta\delta_{ps}$ is always positive for the ipso carbon with increasing cross-linker the $\Delta\delta_{ps}$ is always negative for the ortho and para carbons. The graphs on Pages 49 and 50 displays the chemical shift

difference in chlorobenzene and aniline for the weight percent cross-linked polymer analyzed.

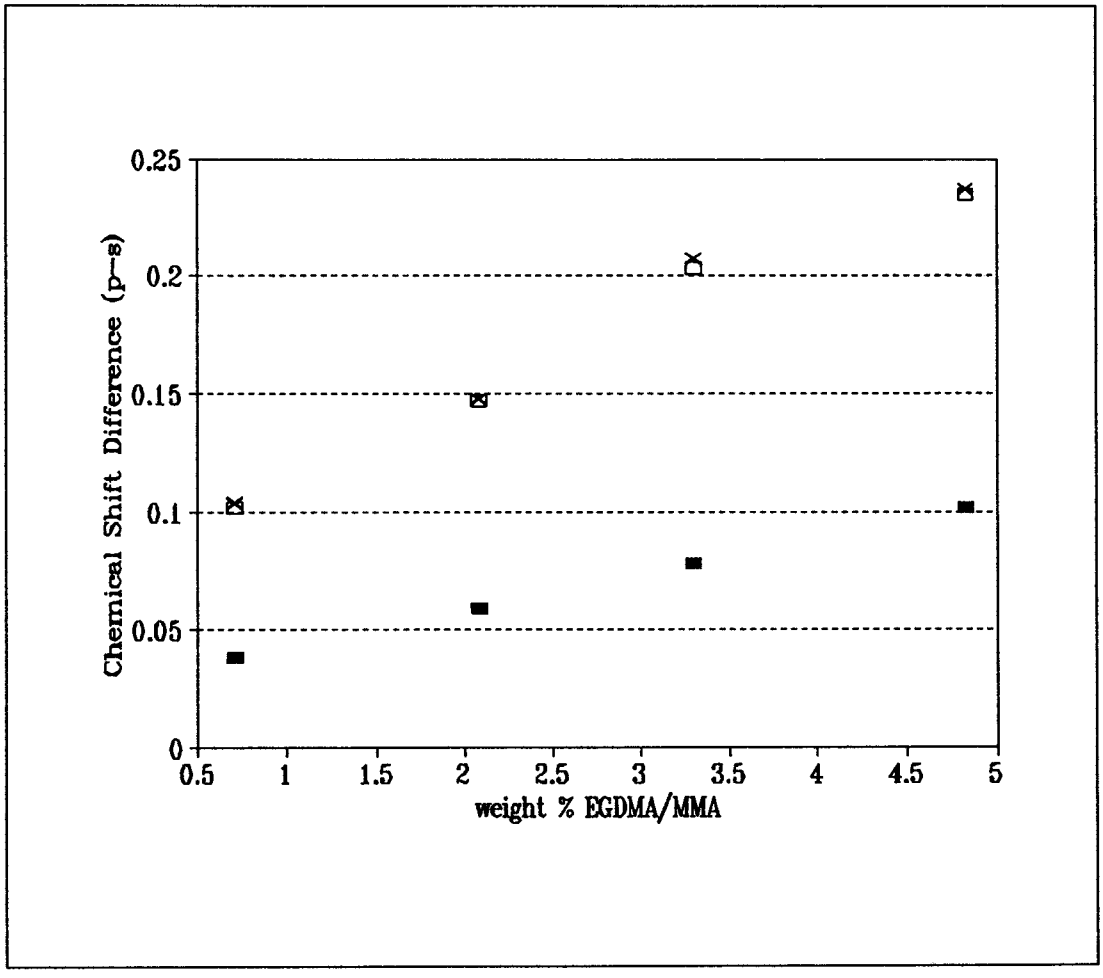

Figure 19. The graph shows the ^{13}C chemical shift difference ($\Delta\delta_{ps}$) for chlorobenzene versus weight percent cross-linker EGDMA in EGDMA/MMA polymer. Different splitting was observed for carbons on the ring; ■ ortho, X meta and □ para.

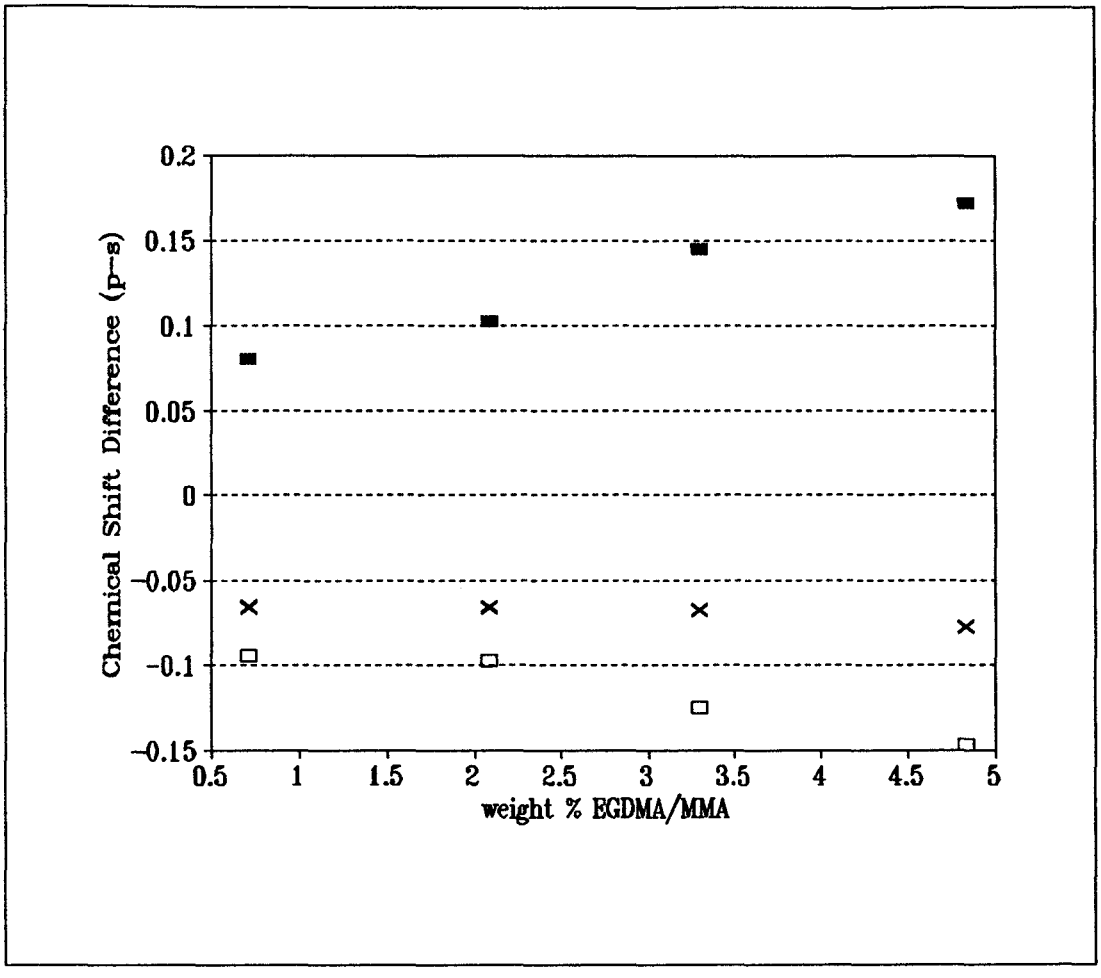

Figure 20. The graph shows the ^{13}C chemical shift difference ($\Delta\delta_{ps}$) for aniline versus weight percent cross-linker EGDMA in EGDMA/MMA polymer. Different splitting was observed for carbons on the ring; ■ ipso, X ortho and □ para.

RELAXATION

The carbon spin-lattice relaxation time constants (T_1) of $CDCl_3$ were determined in 0.7, 2.1 and 4.8 weight percent EGDMA in EGDMA/MMA polymer. The polymer was placed in a 5mm NMR tube with excess $CDCl_3$. The normal ^{13}C spectrum for $CDCl_3$ consists of three lines; the ^{13}C carbon transitions are coupled to the three spin states of deuterium. The presence of the six lines shows that the chloroform occupies two

environments. As mentioned earlier the assignments of the signals were simply done by adjusting the height of the sample in the tube relative to the detection range of the spectrometer. As shown earlier the solvent associated with the polymer occurs at a higher chemical shift than the solvent not associated with the polymer.

Two different T_1 experiments were conducted, the experiments are commonly known as the non-selective and selective inversion-recovery experiments. For the non-selective inversion-recovery experiment a 180° - τ - 90° - Acquire - Delay ($5T_1$) pulse sequence was used. Tau(τ) is a variable delay used to monitor different stages of the relaxation. In the selective inversion recovery experiment the 90° - τ_1 - 90° - τ_2 - 90° - Acquire - Delay ($5T_1$) pulse sequence was employed. The τ_1 is a delay required to cause a selective inversion experiment. The value of τ_1 was equal to inverse of the scalar coupling constant (J_{CD}), or the spacing between the three lines. The τ_1 delay is analogous to the τ in the non-selective inversion experiment. A slight modification had to be employed in the inversion recovery experiment.

In the selective inversion recovery the transmitter frequency is set on the lowest field, highest chemical shift peak. Normally the τ_1 is set equal to the inverse of the frequency difference of the two sites ($1/2\Delta\nu$), however in this experiment τ_1 was set equal to the inverse of the carbon deuterium coupling constant ($1/J_{CD}$). In order to explain this delay we will again consider the magnetization as a vector in the rotating frame. The selective inversion experiment was explained in Chapter 2. Immediately after the 90° pulse the magnetization is in the xy plane. If we incorporate a delay this allows some of the magnetization to evolve in the xy plane. After the time τ_1 ($1/J_{CD}$) the line which

is at a lower chemical shift and is separated by J_{CD} will rotate 360° in the x-y plane, where the signal which separated by $2*J_{CD}$ will rotate 720°. The spacing between the two types of solvents has an substantial effect on the initial conditions of the selective inversion experiment

Consider the spacing between the bound and free solvent lines. At the time of the second 90° pulse, which sets up the selective inversion, the optimum condition is for the bound and free solvent to be 180° out of phase. If the free solvent lines were $J_{CD}/2$ from the bound solvent lines, the lines would be 180° out of phase. For each of the different weight percent cross-linker polymers analyzed, the spacing was optimized by using different spectrometer frequencies. For the 0.7, 2.1, and 4.8 weight percent EGDMA/MMA polymer the spectrometer frequencies used were 50, 62.5, and 125 MHz respectively. Usually the lines were not separated by J_{CD} and only a partial selective inversion was usually accomplished. However at the end of the τ_1 ($1/J_{CD}$) all three components have the same phase, but the components may evolve at different rates.

The ^{13}C T_1's for $CDCl_3$ is on the order of 70 seconds depending on solvent and temperature. Bain *et al*[29] measured the exchange rates in 0.5, 1 and 2 weight percent EGDMA in EGDMA/MMA for $CDCl_3$ to be on the order of $0.01s^{-1}$. They reported that the exchange rate did not change within experimental error. The samples used in their analysis were prepared by bulk polymerization in an ampoule. In the analysis presented in this thesis the polymers were synthesized by bulk polymerization, but this time using a round bottom flask. The T_1 measurements are summarized in Table 10.

4.8 wt % EGDMA/MMA	Nonselective T_1	Selective T_1
bound solvent free solvent	48 (50%) 55 (43%)	11 (60%) Not determined
2 wt% EGDMA/MMA (ampoule)	Nonselective T_1	Selective T_1
bound solvent free solvent	43 (15%) 52 (15%)	28 (38%) Not determined
2.1 wt % EGDMA/MMA	Nonselective T_1	Selective T_1
bound solvent free solvent	52 (10%) 76 (10%)	Not determined Not determined
0.7 wt % EGDMA/MMA	Nonselective T_1	Selective T_1
bound solvent free solvent	67 (10%) 71 (4%)	45 (30%) Not determined

Table 10. The nonselective and selective T_1's for 0.7 wt%, 2.1 wt%, 2 wt% (ampoule synthesis) and 4.8 wt% EGDMA in EGDMA/MMA polymer for the free and bound $CDCl_3$ is shown. The T_1's are given in seconds and the error associated for each of T_1's is shown the brackets for the T_1's that were determined.

The data presented in the table has large error associated with each of the values. The T_1's of the bound solvent decrease with increasing percent cross-linking; this is consistent with Bain *et al*[29]. The exchange rates were not determined because the data were not acceptable for exchange rate calculations. Further information can not be extracted from Table 10 due to the questionable data. The reason for this large error is due to restrictions on the instrument time. As mentioned earlier the ^{13}C T_1 for $CDCl_3$ is about 70 seconds, this results in a delay (τ_1) of 350 seconds between scans. A typical T_1 experiment consists of 12 different variable delays, and 16 scans for each variable delay. The total time for such an experiment would then take about 1 day. The spectra for the T_1's did not have sufficient signal to noise to give acceptable data. The rate of

magnetization transfer between the two sites, usually known as the rate of chemical exchange could be studied by fitting the equations (Equations 7 and 8) described in the theory section.

SOLVENT DEPENDENCE

In a further attempt to describe the origin of the splitting it would be interesting to observe the behaviour of the polymer in different environments or different solvents. The solvents analyzed can be classified into two broad categories, namely aromatic and nonaromatic. The polymer used for the solvent dependence was 4.8% weight percent EGDMA in EGDMA/MMA polymer. The ^{13}C spectra was analyzed to observe the splitting, and to measure the linewidths of each of the signals. As mentioned earlier, swelling measurements may provide information on the nature of the splitting. In addition to acquiring the ^{13}C spectra, swelling measurements were taken.

In the next few pages, the solvent dependence on linewidths, swelling measurements and chemical shift difference will be presented. The linewidths can provide some additional information about the solvent-polymer interactions. The linewidths of the solvent were observed to be broader than the neat solvent. If the broadening is due to a distribution of sites then the broadening will scale as the frequency of the spectrometer. However if the broadening does not scale with spectrometer frequency then another mechanism of broadening may be present. Therefore an easy way to detect whether this mechanism of broadening occurs is to measure the linewidths at different frequencies. The interest of this study was to determine whether this type of broadening occurred, so only two different (50 MHz and 125 MHz) spectrometer

frequencies were used. This analysis will not fully explain all the broadening, but give an indication of the predominant mechanism for broadening. Broadening that scales as the frequency is known as inhomogeneous broadening. If inhomogeneous broadening in these polymer systems is observed then it does not rule out other types of broadening. Broadening that does not scale with the frequency is known as homogenous linebroadening. Table 11, 12 and 13 summarize the solvents affect on 4.8 wt% EGDMA in EGDMA/MMA polymer for the nonaromatic compounds analyzed.

Solvent in 4.8 weight % EGDMA/MMA polymer	Dipole Moment (Debye)	Volume Susceptibility $-\chi_v \times 10^6$	Swelling Percent Increase	Linewidth at half height	
				50MHz	125MHz
CH_3OH	1.7	0.515	0	24	26
C_6H_{12}	0	0.631	0	5	6
$(CH_2OH)_2$	2.28	0.618	0	2	3
CCl_4	0	0.684	20	5	6
CH_3COCH_3	2.88	0.460	70	CH_3 18	43
				CO 17	43

Table 11. The dipole moment, volume susceptibility, swelling measurements of the solvent, and the linewidths at 50 MHz and 125 MHz for nonaromatic solvents that did not show any splitting.

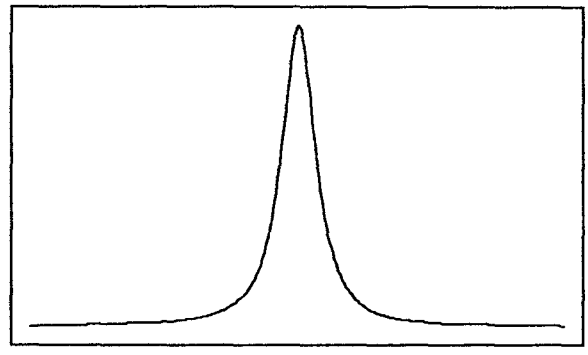

Figure 21. The ^{13}C spectrum of ethylene glycol in 4.8 weight percent EGDMA in EGDMA/MMA polymer at 50 MHz is shown. The frequency range displayed above is 50 Hz (1ppm).

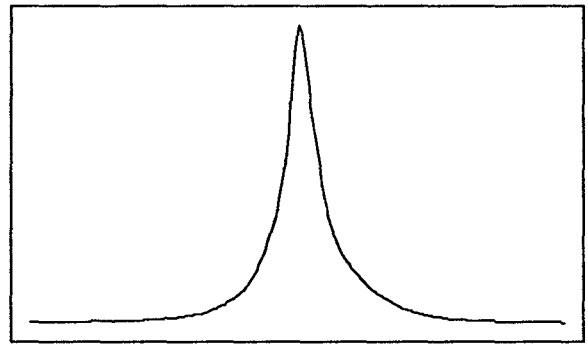

Figure 22. The ^{13}C spectrum of ethylene glycol in 4.8 weight percent EGDMA in EGDMA/MMA polymer at 125 MHz is shown. The frequency range displayed above is 50 Hz (0.4ppm).

The two spectra above display the linewidths for ethylene glycol at different field strengths. If the linewidths are field dependent the linewidths should scale with field strength.

Solvents in 4.8 weight % EGDMA/MMA polymer	Chemical Shift Difference $\Delta\delta_{ps}$ ^{13}C	Dipole Moment (Debye)	Volume Susceptibility $-\chi_v \times 10^6$	Swelling Percent Increase
CH_3I	-0.50	1.62	0.918	115
$ClCH_2CH_2Cl$	0.08	1.90	0.757	170
CH_2Cl_2	0.08	1.60	0.733	210
$CHCl_3$	0.31	1.01	0.735	220

Table 12. The dipole moment, volume susceptibility, swelling measurements of the solvent, and the ^{13}C chemical shift difference ($\Delta\delta_{ps}$) for nonaromatic solvents that did show any splitting. See Table 13 for the linewidths at 50 MHz and 125 MHz for these nonaromatic solvents.

Solvents in 4.8 weight % EGDMA/MMA polymer	Linewidths at half height (Hz)			
	50 MHz		125 MHz	
	free	bound	free	bound
CH_3I	15	15	35	48
$ClCH_2CH_2Cl$	2.5	3	7	12.5
CH_2Cl_2	3	5	6	10
$CHCl_3$	5	7	22	25

Table 13. The linewidths at 50 MHz and 125 MHz for the nonaromatic solvents that did show any splitting.

From the above tables several observations can be noted. The splitting does not seem to depend on the dipole moment of the solvent, however the splitting does seem to depend on the volume susceptibility of the solvent involved. Splitting occurs for solvents in Table 11 and 12 for χ_v below -0.69×10^6, and does not occur for χ_v above -0.69×10^6. This suggests susceptibility may play a part in the splitting of the solvent

signals. In addition the splitting occurs for swelling increases above approximately 100%. The linewidths do not change with frequency for solvents that do not swell very much; less than 20%. Note that for acetone in which the swelling is greater than 70% has linewidths that are frequency dependent and do not split. It appears that once the swelling is greater than 100% the solvent shows two different sites or in other words splits. The ^{13}C linewidths of the solvents that split are frequency dependent for both the bound and free solvents. The ^{13}C chemical shift difference $\Delta\delta_{ps}$ for iodomethane, 1,2 dichloroethane, methylene chloride, and chloroform are -0.50, 0.08, 0.08 and 0.31 respectively. For nonaromatic solvents the solvent-polymer interaction can be summarized as follows. Splitting occurs when the swelling is greater than approximately 100%, and when the swelling is greater than 70% a contribution to the linebroadening is due a to distribution of sites. These limits on the swelling which result in splitting or broadening suggest that both physical and chemical interactions are involved.

The analysis for the aromatic solvents data is summarized in Tables 14 and 15.

Solvents in 4.8 weight % EGDMA/MMA polymer	Dipole Moment (Debye)	Volume Susceptibility $-\chi_v \times 10^6$	Swelling Percent Increase
iodobenzene	1.7	0.826	0
nitrobenzene	4.22	0.598	180
toluene	0.36	0.631	80
benzene	0	0.626	40
o-diclorobenzene	2.5	0.748	30
bromobenzene	1.7	0.771	70
chlorobenzene	1.69	0.707	130
aniline	1.53	0.707	190

Table 14. The dipole moment, volume susceptibility and the swelling measurements of the solvent for aromatic solvents that did show splitting. See Table 15 for the ^{13}C chemical shift difference ($\Delta\delta_{ps}$) and the linewidths at 50 MHz and 125 MHz for the aromatic solvents.

The linewidths and the ^{13}C chemical shift difference ($\Delta\delta_{ps}$) of the aromatic compounds are summarized in Table 15.

Solvents in 4.86 weight % EGDMA/MMA polymer	Carbon #	Chemical Shift Diff. $\Delta\delta_{ps}$	Linewidths at half height			
			50 MHz		125 MHz	
solvent			solvent		solvent	
iodobenzene	C1	NS	10		31	
	C2/6	NS	10		31	
	C3/5	NS	11		33	
	C4	NS	11		31	
nitrobenzene	C1	NS	13		31	
	C2/6	NS	11		33	
	C3/5	NS	12		35	
	C4	NS	11		38	
toluene	C1	NS	18		37	
	C2/6	NS	18		40	
	C3/5	NS	18		44	
	C4	NS	17		39	
	CH_3	NS	17		43	
benzene	All C	NS	13		28	
ortho-dichloro-benzene	C1/2	NS	5		8.5	
	C3/6	NS	6		12	
	C4/5	NA	5		10	
solvent		$\Delta\delta_{ps}$	free	bound	free	bound
bromobenzene	C1	NS	2	NS	3	NS
	C2/6	0.08	1.5	4	5.5	14
	C3/5	0.20	1	6	5	16
	C4	0.20	1	4	4.5	12
chlorobenzene	C1	NS	3.5	NS	8	NS
	C2/6	0.09	3.5	3.5	12	10
	C3/5	0.23	3.5	3.5	10.5	10
	C4	0.23	4.5	3.5	9	9
aniline	C1	0.16	2.5	2.5	7	6
	C2/6	-0.066	2	3	8	6.5
	C3/5	NS	1	NS	8.5	NS
	C4	-0.146	2.5	4	8	7

Table 15. (Previous page) The ^{13}C chemical shift difference ($\Delta\delta_{ps}$) and the linewidths at 50 MHz and 125 MHz for the aromatic solvents. The carbon number indicates the carbon of interest as shown in Figure 10.

For aromatic solvents the system is more complex. For a volume susceptibility smaller than -0.70 x 10^6 splitting occurs for all solvents except iodobenzene. The linewidth dependence differs from the nonaromatic solvents in that most of the aromatic solvent's linewidths are field dependent. The splitting seems less dependent on swelling and is harder to generalize. However splitting occurs for swelling above 70% with the exception of toluene and nitrobenzene. In addition to measuring linewidths as function of solvent, the linewidths of the free and bound were measured for chloroform, methylene chloride, chlorobenzene, bromobenzene, aniline and iodobenzene as a function of the weight percent EGDMA in EGDMA/MMA polymer. Tables 16-21 summarize the data for ^{13}C linewidth measurements for chloroform, methylene chloride, chlorobenzene, bromobenzene, aniline, and iodobenzene.

Weight Percent EGDMA/MMA polymer	Linewidths at half height Carbon		Linewidths at half height Proton	
	free	bound	free	bound
0.7	2	5	9	4
2.1	2	6	15	4.5
3.3	2.5	6	9	8
4.8	2.5	6	15	7
9.2	2.5	9	17	7
16.5	3.5	5.5	13	10

Table 16. The ^{13}C and ^{1}H and linewidths are summarized for the free and bound solvents as function of weight percent EGDMA in EGDMA/MMA polymer in chloroform. The linewidths were measured from spectra taken at 125 MHz and 500 MHz for ^{13}C and ^{1}H respectively.

Weight Percent EGDMA/MMA polymer	Linewidths at half height Carbon		Linewidths at half height Proton	
	free	bound	free	bound
2.1	5	6.5	8	8.5
3.3	5	8.5	17.5	21.5
4.8	6	7.5	13.5	13.5
9.2	10	21.5	21.5	20.5
16.5	8.5	17	25	42

Table 17. The ^{13}C and ^{1}H and linewidths are summarized for the free and bound solvents as function of weight percent EGDMA in EGDMA/MMA polymer in methylene chloride. The linewidths were measured from spectra taken at 125 MHz and 500 MHz for ^{13}C and ^{1}H respectively.

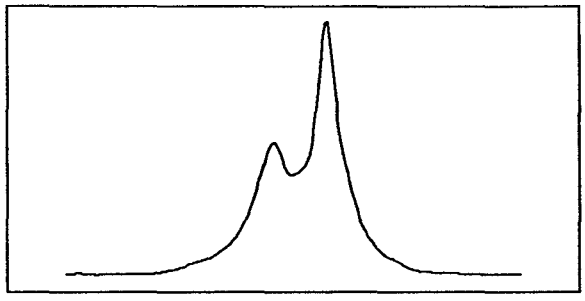

Figure 23. The ^{13}C spectrum of methylene chloride in 2.1 weight percent EGDMA in EGDMA/MMA polymer is displayed.

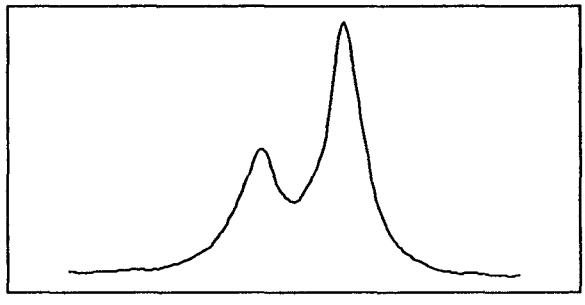

Figure 24. The ^{13}C spectrum of methylene chloride in 4.8 weight percent EGDMA in EGDMA/MMA polymer is displayed.

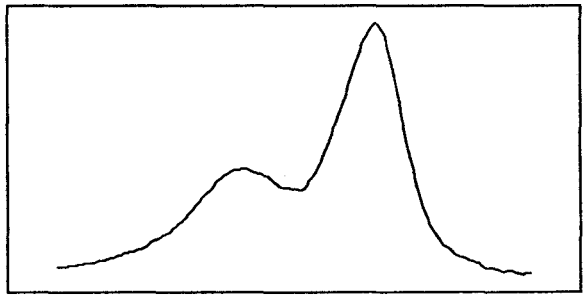

Figure 25. The ^{13}C spectrum of methylene chloride in 9.2 weight percent EGDMA in EGDMA/MMA polymer is displayed.

The above figures illustrate the chemical shift difference and linewidths dependence on the weight percent EGDMA in EGDMA/MMA polymer. Each of the spectra above were acquired at 125 MHz and the frequency range displayed is 75 Hz (0.6ppm).

Weight Percent EGDMA/MMA polymer	Linewidths at half height			
	C1	C2/6	C3/5	C4
0.7	23.5	27.5	29	27
2.1	15.5	28.5	33.5	32
3.3	32	38.5	40.5	38.5
4.8	41.5	56	43.5	42
9.2	36	52.5	38	38.5

Table 18. The ^{13}C linewidths for the carbons at various positions on the ring are summarized for iodobenzene as function of weight percent EGDMA in EGDMA/MMA polymer. The ^{13}C spectra were acquired at 125 MHz.

Weight Percent EGDMA/MMA polymer	Linewidths at half height						
	C1	C2/6		C3/5		C4	
	free	bound	free	bound	free	bound	free
0.7	5	6	6	9	5.5	7	4
2.1	5	7	6	9	5.5	8	4.5
3.3	7	10	9	11	9.5	9	7.5
4.8	8	10	12	10	10.5	9	9
9.2	10	NS	14.5	NS	14.5	NS	11.5
16.5	11.5	NS	16.5	NS	17	NS	12

Table 19. The ^{13}C linewidths for the carbons at various positions on the ring are summarized for chlorobenzene as function of weight percent EGDMA in EGDMA/MMA polymer. The ^{13}C spectra above were acquired at 125 MHz.

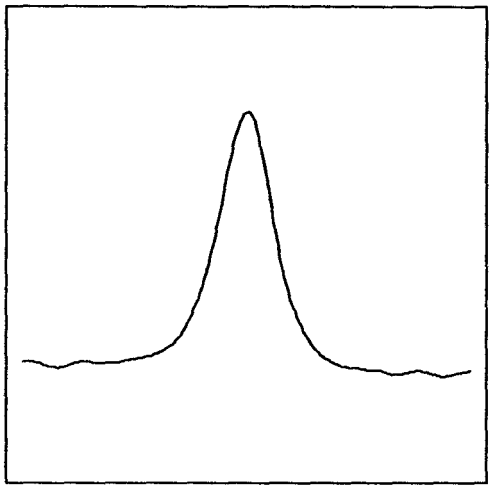

Figure 26. Carbon #1

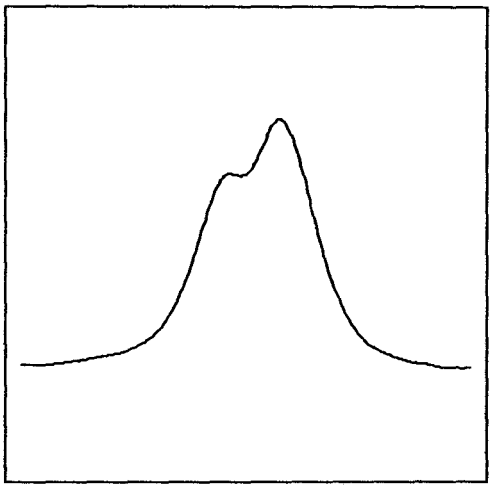

Figure 27. Carbons #2 & #6

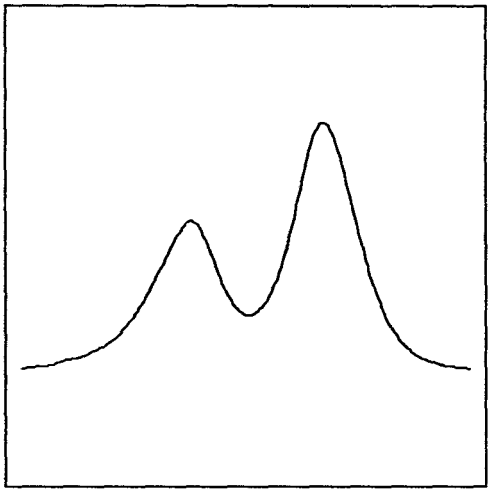

Figure 28. Carbons #3 & #5

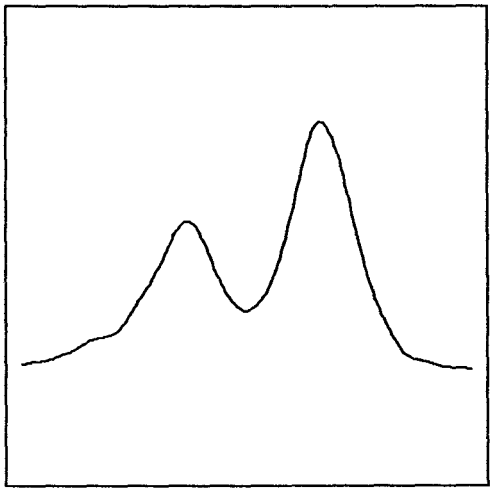

Figure 29. Carbon #4

The above figure displays the solvent splitting for chlorobenzene in 4.8 weight percent EGDMA in EGDMA/MMA polymer at 50 MHz. The ^{13}C spectra shown above are for the four carbon resonances on the ring. Compare the above linewidths with the linewidths in Figures 15-19. The frequency range displayed in all 4 figures is 40 Hz (0.8ppm).

Weight Percent EGDMA/MMA polymer	Linewidths at half height						
	C1	C2/6		C3/5		C4	
	free	bound	free	bound	free	bound	free
0.7	1	7	3	8	2	5.5	2
2.1	5	20	6	27.5	6.5	20	7
3.3	6	16.5	8	19	7.5	15	7.5
4.8	3	14	6	16	6	12	4.5
9.2	4.5	NS	9	NS	7	NS	6.5
16.47	7	NS	13	NS	12	NS	11

Table 20. The ^{13}C linewidths for the carbons at various positions on the ring are summarized for bromobenzene as function of weight percent EGDMA in EGDMA/MMA polymer. The ^{13}C spectra were acquired at 125 MHz.

Weight Percent EGDMA/MMA polymer	Linewidths at half height						
	C1	C2/6		C3/5		C4	
	bound	free	free	bound	free	free	bound
0.7	11	2.5	6.5	8.5	8	5	14
2.1	12.5	7.5	8	8	10	8	10.5
3.3	12	10	12	7.5	12	10	12.5
4.8	6	7	8	6	8.5	8	7.5
9.2	NS	7	11.5	NS	10	10.5	NS
16.5	NS	8	12.5	NS	11	11	NS

Table 21. The ^{13}C linewidths for the carbons at various positions on the ring are summarized for aniline as function of weight percent EGDMA/MMA polymer. The ^{13}C spectra were acquired at 125 MHz.

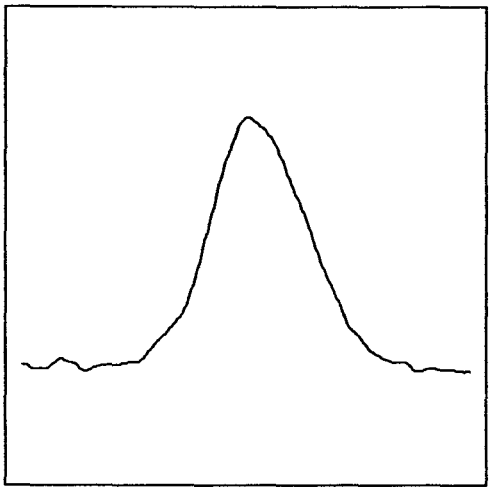

Figure 30. Carbon #1

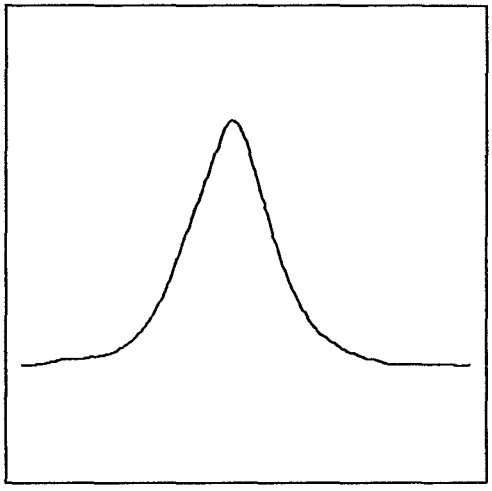

Figure 31. Carbons #2 & #6

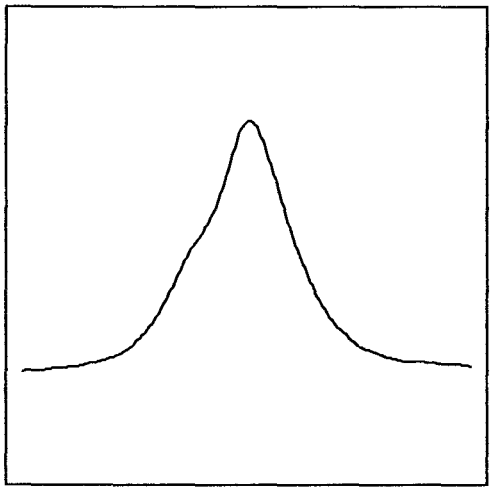

Figure 32. Carbons #3 and #5

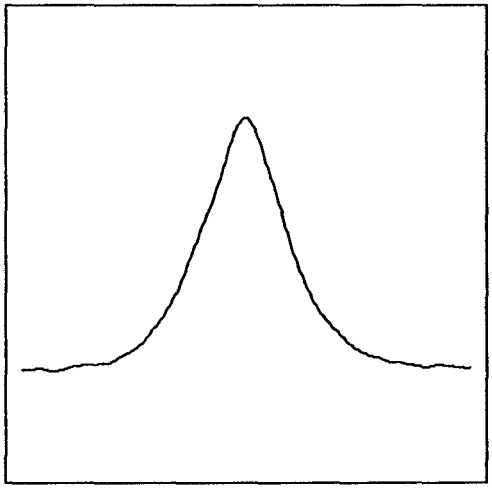

Figure 33. Carbon #4

The above figure displays the solvent splitting for nitrobenzene in 4.8 weight percent EGDMA in EGDMA/MMA polymer at 50 MHz. The ^{13}C spectra are shown for the four carbon resonances on the ring. The frequency range displayed in all 4 figures is 60 Hz (1.2ppm).

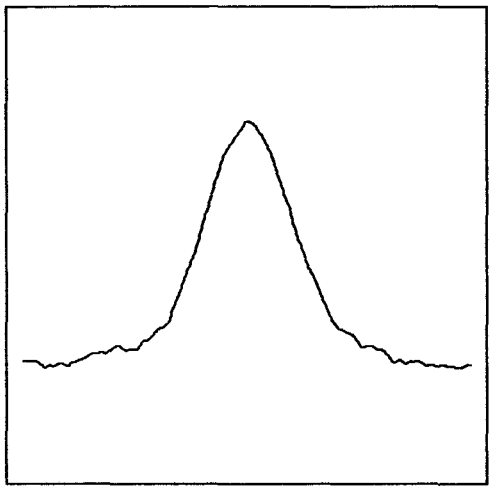

Figure 34. Carbon #1

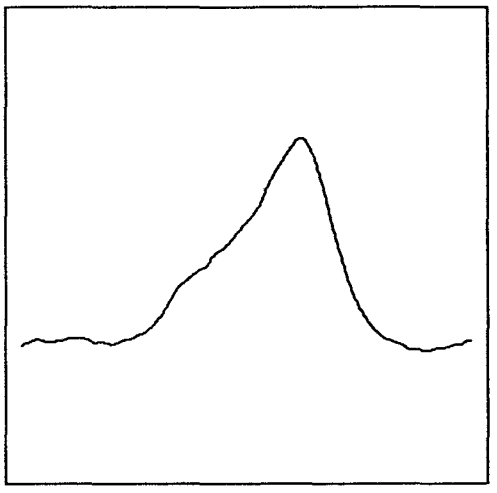

Figure 35. Carbons #2 & #6

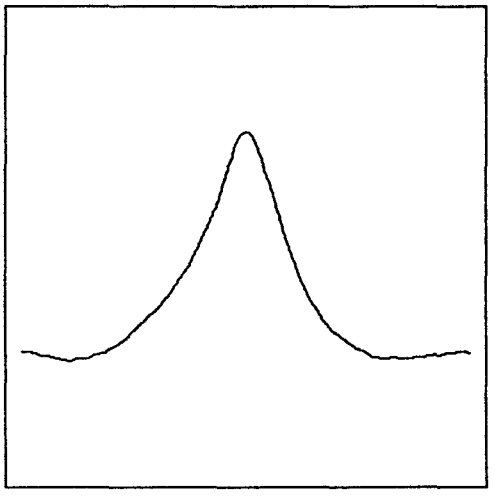

Figure 36. Carbons #3 and #5

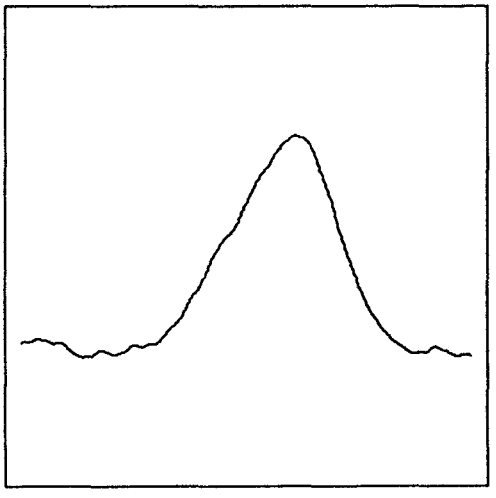

Figure 37. Carbon #4

The above figure displays the solvent splitting for nitrobenzene in 4.8 weight percent EGDMA in EGDMA/MMA polymer at 125 MHz. The ^{13}C spectra are for the four carbon resonances on the ring. The frequency range displayed in all 4 figures is 150 Hz (1.2ppm).

In general as the weight percent EGDMA in EGDMA/MMA polymer increases the linewidths increase. It was shown earlier that one contribution to the linebroadening is due to a distribution of sites. Assuming that the distribution of these sites remains constant as the percent cross-linker increases, and this type of broadening is the dominant mechanism of broadening one would expect that the extent of broadening would remain constant as the cross-linking is varied. In the above tables the broadening, however increases as the percent cross-linker increases. If the above assumption is valid, one can clearly see that another mechanism of broadening must exist.

As shown earlier by swelling measurements, as the percent cross-linker increases, the polymer gets more rigid and more compact. As the polymer becomes more compact it starts to approach solid-like properties. One of the major problems in solid state NMR is that most of the spectra consist of very broad lines. As mentioned earlier this can be due to a number of mechanisms, namely chemical shift anisotropy, dipolar coupling and chemical shift dispersion. In addition not all swollen polymer gels show the same types of broadening. The ^{13}C linewidths of 2% divinylbenzene cross-linked polystyrene beads swollen in deuteriochloroform were shown to have broadening mainly due to chemical shift anisotropy.[44] In contrast the ^{13}C linewidths of poly(sodium acrylate) swollen in water which were broadened by chemical shift dispersion, and the problem of field inhomogeneity.[45] Although it is not of present interest to determine the degree to which these contribute to the broadening they cannot be overlooked.

One further point of interest is that although the linewidths generally increase as the percent cross-linked increases for the majority of the solvents, the linewidths for the

4.8 weight percent decrease. This decrease in linewidth could indicate a change in the linebroadening mechanisms. For example, it could be that the dominant mechanisms of linebroadening do not contribute the same to the total broadening as the amount of cross-linking changes.

The results presented will be used to help understand the solvent-polymer interactions and to determine the nature of the solvent-polymer splitting. A model about the solvent-polymer interactions will be presented based on the experimental data. It is difficult to account for all the experimental data because many effects can be operating at any one time. However this appears to be one of the first attempts to explain solvent splitting of non ion-exchange polymer systems with NMR.

Chapter 4

DISCUSSION

In order to best summarize the results on how the solvent and polymer are interacting, a model will be presented to summarize the results. The total solvent-polymer interaction can be best explained by breaking the interaction into a number of interactions that contribute in different ways to the total effect. There seems to be three different solvent-polymer interactions that are present.

1) A weak chemical interaction exists that causes broadening of most solvents.

2) A stronger chemical interaction that results in the splitting of the solvent signal.

3) A physical interaction that controls the degree of splitting.

The above interactions will now be discussed in terms of the data presented in the results section. The first, the weak chemical interaction, explains the field dependent broadening that is present in most solvents. The solvents that did not show this weak interaction are methanol, cyclohexane, ethylene glycol, carbon tetrachloride, and dichlorobenzene for the 4.8 weight percent EGDMA in EGDMA/MMA polymer. In addition these solvents also showed the least swelling ability. With the exception of benzene all the solvents that exhibited swelling greater than 70% also had a component of broadening that is field

dependent. In the case of benzene the swelling was only 40%, however the broadening was field dependent. This connection between swelling and heterogenous (field dependent) linebroadening supports the belief that the ability of a solvent to cause swelling is dependent on how the solvent is able to interact chemically with the polymer. This type of interaction can be visualized as solvent within the interstices of the polymer. This type of solvent molecule has been referred to as free solvent. More precisely, the term free has been used to refer to solvent not associated with the polymer at all, however free solvent also includes this interstitial solvent.

The stronger chemical interaction is believe to result in the splitting that has been observed. The frequency splitting scales when the field strength is modified, this resembles a chemical shift phenomenon. If the splitting were not field dependent the splitting may be termed as a coupling effect. The coupling effect which is a result of interaction between nuclei. This coupling effect is a physical effect and does not change with field. A chemical shift arises because of the shielding of the nuclei from the external magnetic field by the electrons. Other evidence is available to support the chemical interaction.

Further evidence for a chemical interaction is observed from the values of the chemical shift differences $\Delta\delta_{ps}$. If the splitting was simply due to physical interaction one would expect that for two similar solvents with comparable swelling properties that they would split equally. Two similar solvents of interest are chloroform and methylene chloride, the swelling measurements for 4.8 weight percent EGDMA in EGDMA/MMA polymer are 220% and 210% for chloroform and methylene chloride respectively. The

^{13}C $\Delta\delta_{ps}$ are 0.08 ppm and 0.31 ppm for methylene chloride and chloroform respectively, and the ^{1}H $\Delta\delta_{ps}$ are 0.07 ppm and 0.11 ppm for methylene chloride and chloroform respectively. There is clearly a substantial chemical shift difference between these two solvents. In addition, not all of the splitting has caused the bound solvent to be in a less electronically shielded environment than the free solvent. In the case of iodomethane the ^{13}C $\Delta\delta_{ps}$ has caused the bound solvent to be in a more electronically shielded environment. This also shows that the splitting is caused by a chemical rather than a physical interaction. Interesting splitting behaviour is noted in the splitting of chlorobenzene, bromobenzene and aniline. As shown earlier, all three solvents showed splitting that is not the same for all carbons of the phenyl ring. For chlorobenzene and bromobenzene the position of the carbons on the ring relative to the substituted carbon shows the same splitting behaviour. The carbons ortho, meta and para to the substituted carbon split, however the only carbon that did not split is the substituted carbon. The splitting for the meta and para carbons was observed to the same for chlorobenzene and bromobenzene. In addition the ortho carbon also split but the splitting was greater in bromobenzene than in chlorobenzene for a given weight percent of EGDMA in EGDMA/MMA polymer analyzed. The ^{13}C $\Delta\delta_{ps}$ was always positive, and increased with increasing weight cross-linked EGDMA/MMA polymer. Once the weight percent cross-linker reached 10% no splitting was observed for chlorobenzene, bromobenzene, and aniline. Aniline showed quite different splitting behaviour than chlorobenzene and bromobenzene. The carbons on the ring for aniline split differently than those of chlorobenzene and bromobenzene. The carbons that were split were the ipso (substituted),

ortho and para carbons, but no splitting was observed at the meta carbons. Aniline was the only aromatic solvent analyzed that split at the ipso carbon. In addition aniline was the only aromatic solvent to have negative chemical shift differences. The sign of the ipso $\Delta\delta_{ps}$ was positive, while both the ortho and para carbons exhibited negative $\Delta\delta_{ps}$. The various dependencies cannot be solely due to a physical interaction, therefore it is plausible that a chemical interaction must be present.

Evidence for a chemical interaction can be found through volume (magnetic) susceptibilities considerations. As mentioned earlier, Gordon in 1962 to a first approximation showed that the origin of splitting of water in ion-exchange resins could be explained in terms of the difference in the volume susceptibilities of the solvent and polymer. However in this analysis although the volume susceptibility of the polymers was not determined for the polymer the volume susceptibilities of the solvents that split did not show any noticeable trend.

In particular methylene chloride and chloroform have very similar volume susceptibilities, χ_v is -0.733×10^6 and χ_v is -0.735×10^6 respectively although the chemical shift difference are not very similar. Also in the case of aniline, for the cross-linked polymers that split, the ipso carbons shows a positive chemical shift difference and the ortho and para showed negative chemical shift difference. This effect cannot be easily explained with susceptibility arguments alone.

The third type of solvent polymer interaction is a physical interaction. This interaction is directly related to the compactness of the polymer. As shown earlier a plot of increased swelling versus carbon chemical shift difference for chloroform clearly

showed a linear dependence. Since ethylene glycol dimethacrylate (EGDMA) and methylmethacrylate (MMA) are very similar chemically in the polymer system it is reasonable to assume that just the increased presence of cross-linker would not cause increased splitting. Instead what is believed to happen is that as the polymer becomes more compact, this causes an increase in the physical association between the solvent and the polymer. The actual mechanism of how the polymer increases the chemical shift difference is not known.

From the analysis of this cross-linked polymer a new way of characterizing cross-linked polymers can be developed. Although the increase in percent swelling is a measure of the compactness of the cross-linked polymer, the chemical shift difference can also determine this compactness. This linear dependence of increase percent swelling on the chemical shift difference was valid for the cross-linking percentage analyzed. The range of weight percent cross-linking analyzed was 1 weight percent to 20 weight percent EGDMA in EGDMA/MMA polymer, and the swelling measurement varied for the polymer in chloroform from 100% to 500% However standards are needed that have well defined weight percent cross-linking percentage of the polymer system of interest, in order to use this technique.

This physical interaction is best illustrated with chloroform and methylene chloride solvents. For chloroform and methylene chloride an almost linear dependence of swelling versus chemical shift difference for carbon and proton spectra was observed. Table 22 summarizes the dependence of swelling on chemical shift difference for both carbon and protons.

Solvent	Carbon (ppm/%)	Proton (ppm/%)
CH_2Cl_2	0.00067	0.00033
$CHCl_3$	0.001	0.00025

Table 22. The dependence of the increase percent swelling on the ^{13}C and ^{1}H chemical shift difference is shown for chloroform and methylene in EGDMA/MMA polymer.

From Table 22 one can see that the carbon chemical shift difference is more sensitive to swelling than the proton chemical shift difference for both solvents. In addition, for methylene chloride, the swelling per ppm for protons is double that for carbon, however for chloroform the proton is four times that for carbon. One would expect that if the interactions were all merely physical, the ratios of swelling chemical shift difference sensitivity would be the same.

CONCLUSIONS

The observation of split solvent NMR peaks has been shown to be useful in the study of solvent-polymer interactions. In general, as the weight percent of cross-linker increases, the swelling ability of the polymer decreases, and the chemical shift difference increases. This behaviour has been observed for all solvents analyzed that showed splitting. In addition this trend has been shown to potentially useful in the characterization of cross-linked polymer.

There are three interactions that are present in order to account for the splitting behaviour observed. The three interactions are 1) a weak chemical interaction that causes the broadening of most solvents, 2) a strong chemical interaction that causes the solvent signal to split and 3) a physical interaction that controls the degree of the splitting. These three splittings contribute in different proportions for the different systems analyzed.

Suggestions For Future Work

1. In order to test the validity of using the chemical shift difference to characterize cross-linked polymers, cross-linked samples with known weight percentage cross-linking are needed.

2. In order to analyze the exchange rates of the solvent as a function of cross-linking a more suitable solvent is needed. The solvent used was $CDCl_3$ and the carbon relaxation was used to attempt to measure the exchange rate. Bain *et al* determined the

exchange rates of chloroform to be on the order of 0.01 sec^{-1}. The study of relaxation process is more pronounced when the relaxation rate (T_1^{-1}) and the exchange rate are similar. The problem in the determination of the exchange rate was attributed to the experimental time constraints. This experimental time is dictated by the T_1 of the relaxing nucleus and the signal to noise required in the acquired spectrum. The experimental time can be shortened greatly if a solvent of a shorter T_1 is used. The T_1 of $CDCl_3$ is about 70 seconds, and that if require is solvent that has a shorter T_1 than chloroform and the solvent must also split.

3. In this study only one polymer system was analyzed it would be interesting to see if the solvent-polymer interactions noted here are found in other polymer systems.

4. This study only looked at the solvent-polymer interactions when one solvent was used. It may be useful to investigate the solvent-polymer interactions in solvent mixtures.

5. The differences in solvent splitting between aniline and chlorobenzene could be due to different types of interactiions with the polymer. It is possible that chlorobenzene may associate through the ring and aniline may associate through the nitrogen of the NH_2 group.

6. In general as the swelling percentage of the EGDMA/MMA polymer decreased the chemical shift difference increased. The chemical shift differences seems to be dependent on the concentration of the polymer present per unit of volume. It would be useful to how the chemical shift depends on the concentration of linear poly(methyl-meth acrylate).

REFERENCES

1. E.M. Purcell, H.C. Torrey and R.V. Pound, Phys. Rev. **69**, 37 (1946).

2. F. Bloch, W.W. Hansen and M.E. Packard, Phys. Rev. **69**, 127 (1946).

3. J.K.M. Saunders and B.K. Hunter, *Modern NMR Spectroscopy. A Guide For Chemists*, Oxford University Press, Oxford, 1988.

4. A.E. Derome, *Modern NMR Techniques for Chemistry Research*, Pergamon Press, Oxford, 1988.

5. R.K. Harris, *Nuclear Magnetic Resonance Spectroscopy*, Pitman Books Limited, London, 1983.

6. R.R. Ernst, G. Bodenhausen and A. Wokaun, *Principles of Nuclear Magnetic Resonance in One and Two Dimensions*, Clarendon Press, Oxford, 1987.

7. J.A. Pople, W.G. Schneider and H.J. Bernstein, *High-Resolution Nuclear Magnetic Resonance*, McGraw-Hill Book Company, Inc., New York, 1959.

8. F. Heatly. *Dynamics of Chains in Solution by NMR Spectroscopy*. In: *Comprehensive Polymer Science. Polymer Characterization*, Pergamon Press, Oxford, 1989.

9. V.D. Fedotov and H. Schneider, *Structure and Dynamics of Bulk Polymers by NMR Methods*, Springer-Verlag, Berlin, 1989.

10. J.K. Kwakye, Talanta **32**, 1069 (1985).

11. G. Govil and R.V. Hosur, *Conformations of Biological Molecules*, Springer-Verlag, Berlin, 1982.

12. K. Wüthrich, *NMR in Biological Research: Peptides and Proteins*, North-Holland Publishing Company, Oxford, 1976.

13. K. Wüthrich, *NMR of Proteins and Nucleic Acids*, John Wiley & Sons, Inc., New York, 1986.

14. P.W. Kuchel. *Biological Applications of NMR*. In: *Analytical NMR*, edited by L.D. Field and S. Sternhell. John Wiley & Sons Ltd., Chichester, 1989.

15. J.H. Battocletti, CRC Crit. Rev. Biomed. Eng. **10**, 1 (1983).

16. J.H. Battocletti, CRC Crit. Rev. Biomed. Eng. **11**, 313 (1984).

17. J.H. Battocletti, CRC Crit. Rev. Biomed. Eng. **13**, 311 (1986).

18. P.J.W. Debye, N. Bloembergen, P.J. Flory and F. Bitter, *Lectures in Material Science*, W.A. Benjamin Inc., 1963.

19. C.G. Smith, R.A. Nyquist, B. Smith, J. Pasztor,Jr. and S.J. Martin, Anal. Chem. **63**, 15R (1991).

20. F.A. Bovey. *Structure of Chains by Solution NMR Spectroscopy.* In: *Comprehensive Polymer Science. Polymer Characterization*, Pergamon Press, Oxford, 1989.

21. F. Laupretre, Prog. Polym. Sci. **15**, 425 (1990).

22. H. Saito and I. Ando, Annu. Rep. NMR Spectrosc. **21**, 209 (1989).

23. B.C. Perry and J.K. Koenig, J. Appl. Polym. Sci. Appl. Polym. Symp. **43**, 165 (1989).

24. F.D. Blum, Coll. Surf. **45**, 361 (1990).

25. M. Andreis and J.L. Koenig, Adv. Polym. Sci. **89**, 69 (1989).

26. C. Jones, Nucl. Magn. Reson. **18**, 289 (1989).

27. A.E. Tonelli, *NMR Spectroscopy and Polymer Microstructure. The Conformational Connection*, VCH Publishers, New York, 1989.

28. L.A. Errede, R.A. Newmark and J.R. Hill, Macromolecules **19**, 651 (1986).

29. A.D. Bain, A.E. Hamielec and M. Mlekuz, Macromolecules (1991).(In Press)

30. J.E. Gordon, J. Phys. Chem. **66**, 1150 (1962).

31. W.T. Ford, M. Periyasamy and H.O. Spivey, Macromolecules **17**, 2881 (1984).

32. J.P. DeVilliers and J.R. Parrish, J. Polym. Sci. Part A **2**, 1331 (1964).

33. R.H. Dinius and G.R. Choppin, J. Phys. Chem. **68**, 425 (1964).

34. R.W. Creekmore and C.N. Reiley, Anal. Chem. **42**, 570 (1970).

35. A. Darícková, D. Doskocilová, S. Sevcik and J. Stamberg, J. Polym. Sci. Part B **8**, 259 (1970).

36. D.D. Tao, D. Doskocilová and J. Stamberg, Angew. Makromol. Chem. **38**, 129 (1974).

37. G.L. Marshall and S.J. Wilson, Eur. Polym. J. **24**, 933 (1988).

38. R.W. Creekmore and C.N. Reiley, Anal. Chem. **42**, 725 (1970).

39. M. Periyasamy and W.T. Ford, Reactive Polymers **3**, 351 (1985).

40. D.L. Pavia, G.M. Lampman and G.S. Kriz, *An Introduction to Spectroscopy. A Guide For Students of Organic Chemistry*, Saunders College Publishing, Philadelphia, 1979.

41. D.R. Muhandiram and R.E.D. McClung, J. Magn. Reson. **71**, 187 (1987).

42. L.S. Frankel, J. Phys. Chem. **75**, 1211 (1971).

43. P.J. Flory. *Statistical Thermodynamics of Polymer Solutions*. In: *Princples of Polymer Chemistry*, Cornell University Press, New York, 1953.

44. H.D.H. Stöver and J.M.J. Fréchet, Macromolecules **24**, 883 (1991).

45. A.D. Bain, D.R Eaton, A.E. Hamielec, M. Mlekuz and B.G. Sayer, Macromolecules **22**, 3561 (1989).